Eulerian derivation of non-inertial Navier-Stokes and boundary layer equations for incompressible flow in constant pure rotation

M.L. Combrinck, L.N. Dala, I.I. Lipatov

PII: S0997-7546(15)30067-4
DOI: http://dx.doi.org/10.1016/j.euromechflu.2016.12.012
Reference: EJMFLU 3135

To appear in: *European Journal of Mechanics B/Fluids*

Received date: 1 May 2015
Revised date: 27 December 2016
Accepted date: 27 December 2016

Please cite this article as: M.L. Combrinck, L.N. Dala, I.I. Lipatov, Eulerian derivation of non-inertial Navier-Stokes and boundary layer equations for incompressible flow in constant pure rotation, *European Journal of Mechanics B/Fluids* (2017), http://dx.doi.org/10.1016/j.euromechflu.2016.12.012

Eulerian Derivation of Non-Inertial Navier-Stokes and Boundary Layer Equations for Incompressible Flow in Constant Pure Rotation

M. L. Combrinck[1,*]

University of Pretoria, South Africa

L.N. Dala[2,*]

Northumbria University, United Kingdom

I.I. Lipatov*

Central Aerohydrodynamic Institute, Russian Federation

Abstract

The paper presents an Eulerian derivation of the non-inertial Navier-Stokes equations as an alternative to the Lagrangian fluid parcel approach. To the best knowledge of the authors, this is the first instance where an Eulerian approach is used for such a derivation. This work expands on the work of [1] who derived the incompressible momentum equation in constant rotation for geophysical applications. In this paper the derivation is done for the full set of Navier-Stokes equations in incompressible flow for pure rotation. It is shown that the continuity equation as well as the conservation of energy equation are invariant under transformation from the inertial frame to the rotational frame. From these equations the non-inertial boundary layer equations for flow on a flat plate subjected to rotation is derived in both the Cartesian and cylindrical co-ordinate systems.

Keywords: Rotational Transform, Galilean Transformation, Coriolis force,

*Corresponding author
Email address: madeleine.combrinck@gmail.com (M. L. Combrinck)
[1]also at Flamengro, a Division of Armscor SOC Ltd, South Africa
[2]also at University of Pretoria, South Africa

Centrifugal force,Boundary layer.

2010 MSC: 76U99

1. Introduction

Derivation of the non-inertial Navier-Stokes equations (conservation of mass, momentum and energy) is generally done using a Lagrangian approach [2]. Although this method, when used correctly, leads to a specific set of equations, it does not clearly indicate the origin of the fictitious forces and can lead to misconceptions. The correct set of equations are required for boundary layer analysis, therefore this study firstly considers the form of the non-inertial Navier-Stokes equations before it moves on the non-inertial boundary layer equations.

In deriving the conservation of momentum equation, the general approach entails the modification of Newton's second law to include the fictitious forces as body forces in the same manner as which the gravity force is handled:

$$\sum \mathbf{F} + \sum \mathbf{F}_{\mathbf{fictitious}} = m\mathbf{a} \tag{1}$$

The fictitious forces are derived separately using a point mass method to obtain a relation for the inertial acceleration in terms of the non-inertial acceleration components [3]:

$$\mathbf{a} = \frac{d^2\mathbf{X}}{dt^2} + \dot{\mathbf{\Omega}} \wedge \mathbf{x} + \mathbf{\Omega} \wedge (\mathbf{\Omega} \wedge \mathbf{x}) + \dot{\mathbf{V}} + 2\mathbf{\Omega} \wedge \mathbf{V} \tag{2}$$

These accelerations are multiplied by the density to obtain the momentum form of the fictitious effects and included on the right hand side of the momentum equation.

This approach, although simple and intuitive, is not rigorous and lends itself to mistakes with regards to the nature of the fictitious forces. It has been observed in literature that these fictitious effects are erroneously added in the conservation of energy equation ([4], [5]). This can particularly occur when this Lagrangian approach is used.

The studies that make use of the non-inertial boundary layer equations ([6], [7], [8], [9], [10]) are applied to blade configurations that is approximated as flat

plates. The studies listed did not include the energy equation. The application of blade geometries extend from wind turbines to helicopter rotors and while the Cartesian formulation can be used it is in some instances more appropriate to make use of a Cylindrical co-ordinates system. The Cylindrical formulation are required for applications where axis symmetry is present such as cone flows and other aero-ballistic geometries.

[1] proposed an Eulerian method for the derivation of the Coriolis and Centrifugal forces in the momentum equation. The derivation was limited to the incompressible conservation of momentum equation in pure rotation. The application of the work was in the Geophysical field. In this paper the work is expanded upon to include the full set of Navier-Stokes equations for incompressible flow in pure rotation.

In most studies, the non-inertial conservation of mass and momentum equations are not explicitly derived ([6], [7], [9]). The equations are merely stated and used in subsequent analysis. No mention is made of the conservation of energy equation. [10] and [8] cited the *Lagrangian method* of derivation used in [2]. In this study the *Eulerian method* is used to derive the non-inertial conservation of mass, momentum and energy equations.

One study was found that investigated the effect of non-inertial reference frames on the conservation of energy equation [11]. This article made use of a point mass method to indicate that the energy and work in a non-inertial system remain invariant. The total energy and work of the system was used here and was therefore not applied to the partial differential conservation of energy equation.

The resulting boundary layer equations were solved using a combination of parametric methods [6], perturbation methods [8] and numerical solution of similarity equations [9], [10]. In this study the boundary layer are resolved directly using the finite volume method.

In this paper the non-inertial equations are derived in vector form using a series of frame transformations. These equations are implemented in a finite volume solver. Validation simulations are conducted for the rotating disk [12]

as described in [13].

The vector equations are subjected to an order of magnitude analysis to obtain the general boundary layer equations. This is done for Cartesian and Cylindrical co-ordinates. These equations are used to describe the behaviour of the boundary layer.

2. Frame Transformations

Assume that three (3) frames exist; O, O' and $\hat{O}$ as indicated in Figure 1. Frame O is the stationary, inertial frame. Frame O' is an orientation preserving frame(**i** and **i**' has the same orientation), which can be either inertial or non-inertial depending on the cases analysed. This frame shares an origin with the rotational frame $\hat{O}$. Frame $\hat{O}$ is the non-inertial, rotational frame and is therefore not orientation preserving.

Now consider a point P which can be observed from all the frames. Point P is rotating around the origin of frame O, but it is stationary in frames O' and $\hat{O}$. The set of equations will be developed to describe the motion of point P in the rotational frame $\hat{O}$.

Figure 1: Frame Descriptions

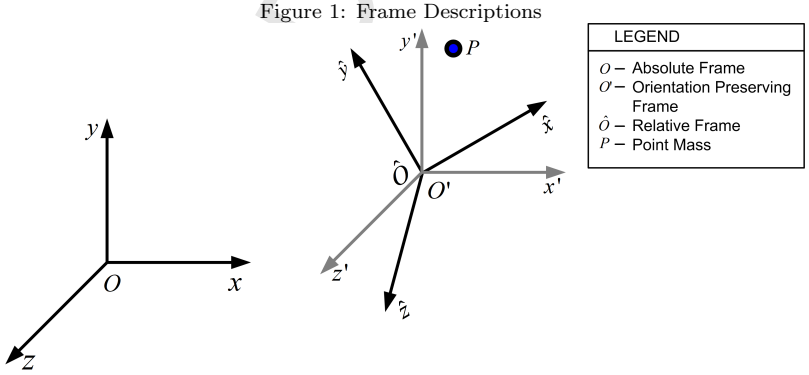

This point is described in frame O from where a local Galilean transformation, $G^{\mathbf{M}}$, will be used to describe it in frame O'. The rotational transform, $R^{\Omega t}$, will then be used to transform the resulting equations (as described in frame O') to the rotational frame $\hat{O}$.

2.1. Local Galilean Transformation

The standard Galilean transform is limited in its application to constant translation velocity vectors. [1] modified it to accommodate constant rotational conditions.

The Galilean transform is used to transform between two reference frames that only differ by a constant vector of motion. In Figure 2 such a motion is described between frame O and O'.

Assume that the origins of the two frames intersect at time $t = 0$ and that frame O' is moving at a constant velocity $\mathbf{V}$ in the x-direction. At time $t = \Delta t$, the frames O and O' are then distance x_{rel} from each other.

Figure 2: Galilean Transformation between Frames

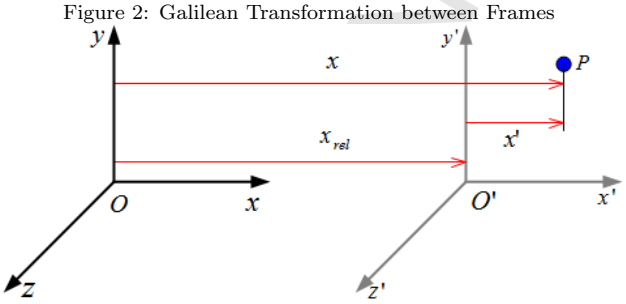

The relationship between the co-ordinates points for this single event between frames O and O' is described by Equation 3. This is known as the standard Galilean transform.

$$\begin{aligned} x' &= x - V\Delta t \\ y' &= y \\ z' &= z \\ t' &= t \end{aligned} \tag{3}$$

Let's further assume at this point that the constant motion need not be in the x-direction alone and that it can be presented as a vector of motion as shown in Figure 3. Let's further assume that it can be used to describe constant motion in rotation as well.

Figure 3: Modified Galilean Transformation between Frames

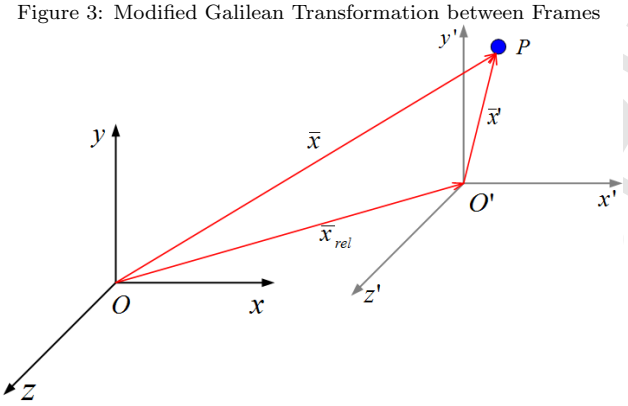

In order to simplify this case let all the frames share the same origin and let the point P be stationary in the rotational frame $\hat{O}$. Therefore point P is rotating with a constant angular velocity around the origin or the inertial frame O. The $\mathbf{x_{rel}}$ component can then be described as:

$$\mathbf{x_{rel}} = \mathbf{V}\Delta t \tag{4}$$

where

$$\mathbf{V} = \mathbf{\Omega} \wedge \mathbf{x} \tag{5}$$

The local Galilean transform operator is introduced such that any vector observed from the inertial frame O can be related to the vector observed from the orientation preserving frame O' as:

$$\mathbf{u}'(\mathbf{x}', t) = G^{\mathbf{M}}\mathbf{u}(\mathbf{x}, t) \tag{6}$$

This definition will lead to a mathematical description to directly relate the vector fields in the inertial frame O, to the vector fields in the orientation preserving frame O':

$$\begin{aligned} \mathbf{u}'(\mathbf{x}', t) &= G^{\mathbf{M}}\mathbf{u}(\mathbf{x}, t) \\ &= G^{\mathbf{\Omega}\wedge\mathbf{x}}\mathbf{u}(\mathbf{x}, t) \\ &= \mathbf{u}(\mathbf{x}, t) + \mathbf{x} \wedge \mathbf{\Omega} \end{aligned} \tag{7}$$

2.2. Rotational Transform

In order to simplify this derivation the assumption will be made that for this specific case all the frames share a common origin. Since frame $\hat{\text{O}}$ shares an origin with the frame O' the vector components in $\hat{\text{O}}$ is related to O' by defining a rotational transform, $R^{\Omega t}$. Equation 7 can be used to describe a vector as seen from frame $\hat{\text{O}}$ in relation to a vector in frame O.

$$\begin{aligned} \hat{\mathbf{u}}(\hat{\mathbf{x}}, t) &= R^{\Omega t}\mathbf{u}'(\mathbf{x}', t) \\ &= R^{\Omega t} G^{\mathbf{\Omega}\wedge\mathbf{x}}\mathbf{u}(\mathbf{x}, t) \end{aligned} \tag{8}$$

$R^{\Omega t}$ is therefore the rotational transform that operates on $\mathbf{x}'$ to obtain the $\hat{\mathbf{x}}$ co-ordinates in the rotational frame. From Equations 7 and 8 it can be derived that for the velocity vector the following relation holds:

$$\hat{\mathbf{u}}(\hat{\mathbf{x}}, t) = R^{\Omega t}\{\mathbf{u}(\mathbf{x}, t) + \mathbf{x} \wedge \mathbf{\Omega}\} \tag{9}$$

Let's assume, for convenience sake, that the rotation is around the z-axis of frame O. The vector $\mathbf{\Omega}$ is then described as $\mathbf{\Omega} = (0, 0, \Omega)$. The rotational transform in this case will be described by the following tensor:

$$R^{\Omega t} = \begin{bmatrix} \cos\Omega t & \sin\Omega t & 0 \\ -\sin\Omega t & \cos\Omega t & 0 \\ 0 & 0 & 1 \end{bmatrix} \tag{10}$$

The first column of this tensor is the projection of the $\mathbf{x}'$ component on $\hat{\mathbf{x}}$,$\hat{\mathbf{y}}$ and $\hat{\mathbf{z}}$. In the same manner is the second and third columns the projection of $\mathbf{y}'$ and $\mathbf{z}'$ respectively on the rotational axes. The quantitative values of the rotation tensor will be different for each case.

Now that the local Galilean invariance and the rotational transform has been described for constant rotational conditions, both can be used in the derivation of the non-inertial Navier-Stokes equations for constant rotation.

3. Transformation of the Navier-Stokes Equations

In this section the non-inertial Navier-Stokes equations for conservation of mass, momentum and energy for constant rotation in incompressible flow will

be derived using an Eulerian approach.

3.1. Conservation of Momentum Equation

The non-inertial momentum equation for incompressible flow in constant rotation was previously derived by [1]. The method is shown in Appendix A for the purpose of enhancing the understanding of the subsequent sections.

The inertial equation for incompressible momentum conservation is describe by the equation below [3]:

$$\frac{\partial \mathbf{u}}{\partial t} + (\mathbf{u} \cdot \nabla)\mathbf{u} = -\nabla\psi + \nu\nabla^2\mathbf{u} \tag{11}$$

where

$$\psi = \frac{p}{\rho} \tag{12}$$

Transformation of the temporal term, according to the method of [1], indicates that the first part of the Coriolis term originates from this transformation:

$$\frac{\partial \hat{\mathbf{u}}}{\partial t}(\hat{\mathbf{x}}_t, t) = R^{\Omega t}[\frac{\partial}{\partial t} + (\boldsymbol{\Omega} \wedge \mathbf{x}) \cdot \nabla - \underbrace{\boldsymbol{\Omega}\wedge]}_{\text{Coriolis}}(\mathbf{u}(\mathbf{x}_t, t)) \tag{13}$$

Similarly, the origin of the of second part of the Coriolis term and the centrifugal term originates from the transformation of the advection term.

$$(\hat{\mathbf{u}} \cdot \hat{\nabla})\hat{\mathbf{u}} = R^{\Omega t}[(\mathbf{u} \cdot \nabla)\mathbf{u} + ((\mathbf{x} \wedge \boldsymbol{\Omega}) \cdot \nabla)\mathbf{u} + \underbrace{(\mathbf{u} \wedge \boldsymbol{\Omega})}_{\text{Coriolis}} - \underbrace{(\mathbf{x} \wedge \boldsymbol{\Omega}) \wedge \boldsymbol{\Omega}}_{\text{Centrifugal}}] \tag{14}$$

In the derivation of Appendix A it is shown that the non-inertial form of the momentum equation is:

$$\frac{\partial \hat{\mathbf{u}}}{\partial t} + (\hat{\mathbf{u}} \cdot \hat{\nabla})\hat{\mathbf{u}} = -\hat{\nabla}\hat{\psi} + \nu\hat{\nabla}^2\hat{\mathbf{u}} + \underbrace{2\hat{\mathbf{u}} \wedge \boldsymbol{\Omega}}_{\text{Coriolis}} - \underbrace{\hat{\mathbf{x}} \wedge \boldsymbol{\Omega} \wedge \boldsymbol{\Omega}}_{\text{Centrifugal}} \tag{15}$$

It can be seen from the equation above that the fictitious forces associated with constant rotation is the Coriolis and centrifugal effects. The centrifugal effect originates from the transformation of the advection term while the Coriolis effect is form both the transient and advection terms.

3.2. Continuity Equation

The conservation of mass, known as the continuity equation, in the inertial frames takes the form [3]:

$$\frac{\partial \rho}{\partial t} + (\nabla \cdot \rho \mathbf{u}) = 0 \tag{16}$$

The first term represents the temporal change in density due to compressibility of the flow. Since this case involves incompressible flow this term can be neglected, but for the purposes of the derivation it will remain in the equation until the last step. The second term is the divergence of density and velocity which represents the residual mass flux of a given control volume.

The non-inertial form of the unsteady density term can be described as:

$$\frac{\partial \hat{\rho}}{\partial t}(\hat{\mathbf{x}}_t, t) = \lim_{\Delta t \to 0} \frac{\hat{\rho}(\hat{\mathbf{x}}_{t+\Delta t}, t + \Delta t) - \hat{\rho}(\hat{\mathbf{x}}, t)}{\Delta t} \tag{17}$$

A Taylor series expansion of the term $\hat{\rho}(\hat{\mathbf{x}}_{t+\Delta t}, t + \Delta t)$ will provide a similar result as shown in Appendix A:

$$\hat{\rho}(\mathbf{x}_{t+\Delta t}, t + \Delta t) = \hat{\rho}(\mathbf{x}_t, t) + [\Delta t(\mathbf{\Omega} \wedge \mathbf{x}) \cdot \nabla]\hat{\rho}(\mathbf{x}_t, t) + (\Delta t \frac{\partial}{\partial t})\hat{\rho}(\mathbf{x}_t, t) \tag{18}$$

Substitution of this expansion in the Equation 17 and manipulation result in an expression that relates the non-inertial, unsteady density to the inertial frame.

$$\frac{\partial \hat{\rho}}{\partial t} = R^{\Omega t}\big[\frac{\partial \rho}{\partial t} + (\mathbf{\Omega} \wedge \mathbf{x}) \cdot \nabla \rho\big] \tag{19}$$

The second term of the continuity equation will be affected by both frame transformations since it contains the velocity vector:

$$\begin{aligned} (\hat{\nabla} \cdot \hat{\rho}\hat{\mathbf{u}}) &= R^{\Omega t} G^{\mathbf{\Omega} \wedge \mathbf{x}} (\nabla \cdot \rho \mathbf{u}) \\ &= R^{\Omega t}[\nabla \cdot \rho (G^{\mathbf{\Omega} \wedge \mathbf{x}} \mathbf{u})] \end{aligned} \tag{20}$$

Equation 9 is used to complete the local Galilean transformation, and the equation becomes:

$$\begin{aligned} (\hat{\nabla} \cdot \hat{\rho}\hat{\mathbf{u}}) &= R^{\Omega t}[\nabla \cdot \rho(\mathbf{u} + \mathbf{x} \wedge \mathbf{\Omega})] \\ &= R^{\Omega t}[\nabla \cdot (\rho \mathbf{u}) + \nabla \cdot \rho(\mathbf{x} \wedge \mathbf{\Omega})] \end{aligned} \tag{21}$$

The equation can be manipulated to the convenient form where the second term is of equal size and opposite sign on the second term in Equation 19.

$$\hat{\nabla} \cdot \hat{\rho}\hat{\mathbf{u}} = R^{\Omega t}[\nabla \cdot (\rho \mathbf{u}) - (\mathbf{\Omega} \wedge \mathbf{x}) \cdot \nabla \rho] \tag{22}$$

The addition of Equation 19 and Equation 22 leads to a relation between the continuity equation in the inertial and rotational frames:

$$\frac{\partial \hat{\rho}}{\partial t} + \hat{\nabla} \cdot \hat{\rho}\hat{\mathbf{u}} = R^{\Omega t}[\frac{\partial \rho}{\partial t} + \nabla \cdot (\rho \mathbf{u})] \tag{23}$$

The right hand side of the equation is equal to zero since this represents the continuity equation in the inertial frame (Equation 16):

$$\frac{\partial \hat{\rho}}{\partial t} + \hat{\nabla} \cdot \hat{\rho}\hat{\mathbf{u}} = 0 \tag{24}$$

Since this is the incompressible case, the temporal term is equal to zero. The continuity equation for the rotational frame therefore takes the form:

$$\hat{\nabla} \cdot \hat{\rho}\hat{\mathbf{u}} = 0 \tag{25}$$

The physical meaning of this equation describes the very nature of incompressible flow assumption; the residual mass flux in a specific control volume is zero. This means that there are no compressible effects in the flow because the same amount of mass flux that enters a domain will exit it. The transient density term causes a change in the residual mass flux in the domain that manifests itself in the form of compressibility.

3.3. Conservation of Energy Equation

The energy equation in the inertial frame takes the following form [3]:

$$\frac{\partial \rho e}{\partial t} + \mathbf{u} \cdot \nabla(\rho e) = -p(\nabla \cdot \mathbf{u}) + \nabla \cdot (k \nabla T) + \Phi \tag{26}$$

The time dependant term is transformed in a similar manner as shown in section 3.2 where the continuity equation was derived. The first term is therefore transformed and the non-inertial component becomes:

$$\frac{\partial \hat{\rho}\hat{e}}{\partial t} = R^{\Omega t}\big[\frac{\partial \rho e}{\partial t} + (\mathbf{\Omega} \wedge \mathbf{x}) \cdot \nabla(\rho e)\big] \tag{27}$$

The convective term is transformed between the frames with the use of the rotational transform, local Galilean transform and substitution of Equation 9

$$\begin{aligned}\hat{\mathbf{u}}\cdot\hat{\nabla}(\hat{\rho}\hat{e}) &= R^{\Omega t}G^{\boldsymbol{\Omega}\wedge\mathbf{x}}\mathbf{u}\cdot\nabla(\rho e)\\ &= R^{\Omega t}[(\mathbf{u}+\mathbf{x}\wedge\boldsymbol{\Omega})\cdot\nabla(\rho e)]\\ &= R^{\Omega t}[\mathbf{u}\cdot\nabla(\rho e)-(\boldsymbol{\Omega}\wedge\mathbf{x})\cdot\nabla(\rho e)] \qquad (28)\end{aligned}$$

The terms that represents the rate of work done by the normal pressure forces is transform between the frames and Equation 9 is inserted:

$$\begin{aligned}-\hat{p}(\hat{\nabla}\cdot\hat{\mathbf{u}}) &= R^{\Omega t}G^{\boldsymbol{\Omega}\wedge\mathbf{x}}[-p(\nabla\cdot\mathbf{u})]\\ &= R^{\Omega t}[-p\nabla\cdot(\mathbf{u}+\mathbf{x}\wedge\boldsymbol{\Omega})]\\ &= R^{\Omega t}[-p\nabla\cdot\mathbf{u}-p\nabla\cdot(\mathbf{x}\wedge\boldsymbol{\Omega})] \qquad (29)\end{aligned}$$

The diffusion is invariant under transformation since the heat transfer coefficient (k) and temperature (T) are scalars. The transformation between the frames then becomes:

$$\begin{aligned}\hat{\nabla}\cdot(\hat{k}\hat{\nabla}\hat{T}) &= R^{\Omega t}G^{\boldsymbol{\Omega}\wedge\mathbf{x}}[\nabla\cdot(k\nabla T)]\\ &= R^{\Omega t}[\nabla\cdot(k\nabla T)] \qquad (30)\end{aligned}$$

The parameter Φ is a scalar value that represents the rate at which mechanical energy is expended in the process of deformation of the fluid due to viscosity [14]. This property, in component form, can be described by:

$$\begin{aligned}\tau:\nabla\mathbf{u} = 2\mu\left[\left(\tfrac{\partial u}{\partial x}\right)^2+\left(\tfrac{\partial v}{\partial y}\right)^2+\left(\tfrac{\partial w}{\partial z}\right)^2-\tfrac{1}{3}(\nabla\cdot\mathbf{u})^2\right]\\ +\mu\left[\left(\tfrac{\partial v}{\partial x}+\tfrac{\partial u}{\partial y}\right)^2+\left(\tfrac{\partial w}{\partial y}+\tfrac{\partial v}{\partial z}\right)^2+\left(\tfrac{\partial u}{\partial z}+\tfrac{\partial w}{\partial x}\right)^2\right] \qquad (31)\end{aligned}$$

The above equation indicates that the dissipation function is a scalar and therefore invariant under transformation:

$$\begin{aligned}\hat{\Phi} &= R^{\Omega t}G^{\boldsymbol{\Omega}\wedge\mathbf{x}}\Phi\\ &= R^{\Omega t}\Phi \qquad (32)\end{aligned}$$

All the transformed terms of the energy equation is summed to obtain the equation below.

$$\frac{\partial \hat{\rho}\hat{e}}{\partial t} + \hat{\mathbf{u}} \cdot \hat{\nabla}(\hat{\rho}\hat{e}) + \quad \hat{p}(\hat{\nabla} \cdot \hat{\mathbf{u}}) - \hat{\nabla} \cdot (\hat{k}\hat{\nabla}\hat{T}) + \hat{\Phi} = R^{\Omega t}[\frac{\partial \rho e}{\partial t} + \mathbf{u}\nabla \cdot (\rho e) + p(\nabla \cdot \mathbf{u}) - \nabla \cdot (k\nabla T) + \Phi] \tag{33}$$

The right hand side of the equation is equal to zero, as shown in Equation 26. The energy equation in the non-inertial frame for constant rotation is invariant under transformation in this specific case:

$$\frac{\partial \hat{\rho}\hat{e}}{\partial t} + \hat{\mathbf{u}} \cdot \hat{\nabla}(\hat{\rho}\hat{e}) = -\hat{p}(\hat{\nabla} \cdot \hat{\mathbf{u}}) + \hat{\nabla} \cdot (\hat{k}\hat{\nabla}\hat{T}) + \hat{\Phi} \tag{34}$$

This equation can be further simplified with the assumption of incompressibility and using Equation 25:

$$\frac{\partial \hat{\rho}\hat{e}}{\partial t} + (\hat{\nabla} \cdot \hat{\rho}\hat{e}\hat{\mathbf{u}}) = \hat{\nabla} \cdot (\hat{k}\hat{\nabla}\hat{T}) + \hat{\Phi}_I \tag{35}$$

Note that the energy equation is invariant under transformation. The lack of fictious work and energy terms in the non-inertial frame was confirmed by [11] by using a point mass model.

4. Non-Inertial Boundary Layer Equations for a Flat Plate in Rotation - Cartesian Formulation

In this next section the non-inertial conservation of mass and momentum equations will be used to derive the non-inertial boundary layer equations for a flat plate subjected to rotations.

Significant work was done by [15] to characterize the laminar boundary layer in turbomachinery applications. The figure below indicates the notation from [15] that will be used in this derivation. The boundary layer develops along the $\hat{x}$- and $\hat{z}$- directions and the rotations assumes constant values along all the axis of rotations.

Figure 4: Flow over a Rotation Flat Surface [15]

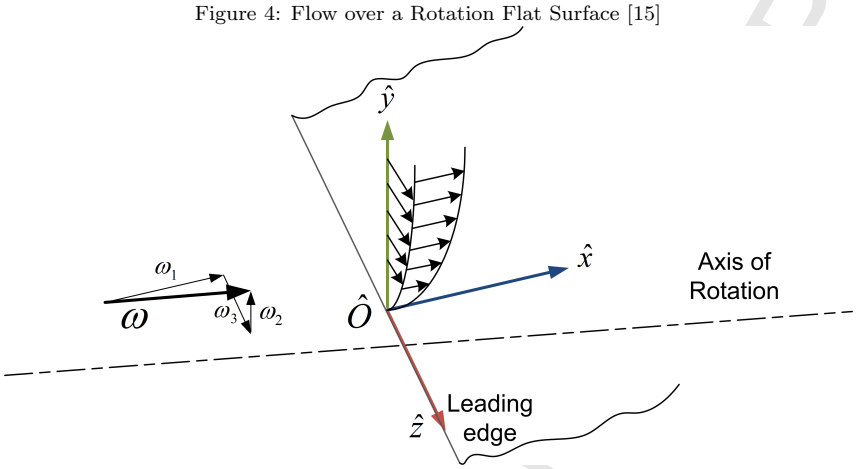

4.1. Non-Dimensional Parameters for Semi-Infinite Flat Plate

The non-dimensional parameters that is selected for the spatial variables is as follow:

$$\begin{aligned} x^\star &= \frac{\hat{x}}{L} \\ y^\star &= \frac{\hat{y}}{\delta} \\ z^\star &= \frac{\hat{z}}{L} \end{aligned} \tag{36}$$

L is the reference distance, the assumption is made that the plate is infinite in the $\hat{x}$- and $\hat{z}$-directions. δ is the boundary layer height in the $\hat{y}$-direction as a distance of L.

The velocity components are non-dimensionalized as follow, where U is the characteristic velocity:

$$\begin{aligned} u^\star &= \frac{\hat{u}}{U} \\ v^\star &= \frac{\hat{v}}{U}\frac{L}{\delta} \\ w^\star &= \frac{\hat{w}}{U} \\ t^\star &= t\frac{U}{L} \end{aligned} \tag{37}$$

The angular velocity can be non-dimensionalized by multiplying it by t.

The units of angular velocity is rad/s, but since radians are already a non-dimensional quantity it can be normalized in this manner.

$$\omega_i{}^\star = \omega_i t \tag{38}$$

The specific pressure and kinematic viscosity can be normalized as follow:

$$\begin{aligned} \psi^\star &= \frac{\psi}{U^2} \\ \nu^\star &= \frac{\nu}{\nu_\infty} \end{aligned} \tag{39}$$

4.2. Continuity Equation for Boundary Layer Flows

The non-inertial continuity equation was derived in previous sections of this paper:

$$\frac{\partial \hat{u}}{\partial \hat{x}} + \frac{\partial \hat{v}}{\partial \hat{y}} + \frac{\partial \hat{w}}{\partial \hat{z}} = 0 \tag{40}$$

Applying the normalization parameters to this equation results in the non-dimensional form of the equation:

$$\frac{\partial (u^\star U)}{\partial (x^\star L)} + \frac{\partial (v^\star \frac{U\delta}{L})}{\partial (y^\star \delta)} + \frac{\partial (w^\star U)}{\partial (z^\star L)} = 0 \tag{41}$$

The equation above is multiplied by:

$$\frac{L}{U} \tag{42}$$

leading to the final non-dimensional form of the equation:

$$\frac{\partial u^\star}{\partial x^\star} + \frac{\partial v^\star}{\partial y^\star} + \frac{\partial w^\star}{\partial z^\star} = 0 \tag{43}$$

No terms can be neglected from this equation and boundary layer continuity equation thus remains the same:

$$\frac{\partial \hat{u}}{\partial \hat{x}} + \frac{\partial \hat{v}}{\partial \hat{y}} + \frac{\partial \hat{w}}{\partial \hat{z}} = 0 \tag{44}$$

4.3. Conservation of Momentum Equation for Boundary Layer Flows

The non-inertial conservation of momentum equation (Equation 15) must be broken up into its direction components in order to treat the principle directions separately. The $\hat{x}$-direction is specified as the first principle directions, and the $\hat{y}$- and $\hat{z}$-direction the second and third respectively.

4.3.1. First Principle Direction Equation

The non-inertial conservation of momentum equation in the $\hat{x}$-direction is as follows:

$$\begin{aligned}\frac{\partial \hat{u}}{\partial t} + \hat{u}\frac{\partial \hat{u}}{\partial \hat{x}} + \hat{v}\frac{\partial \hat{u}}{\partial \hat{y}} + \hat{w}\frac{\partial \hat{u}}{\partial \hat{z}} &= -\frac{\partial \hat{\psi}}{\partial \hat{x}} + \nu(\frac{\partial^2 \hat{u}}{\partial \hat{x}^2} + \frac{\partial^2 \hat{u}}{\partial \hat{y}^2} + \frac{\partial^2 \hat{u}}{\partial \hat{z}^2}) \\ &+ 2\hat{v}\omega_3 - 2\hat{w}\omega_2 \\ &+ \hat{x}({\omega_3}^2 + {\omega_2}^2) - \hat{y}\omega_1\omega_2 - \hat{z}\omega_1\omega_3\end{aligned} \tag{45}$$

By implementing the normalization parameters and multiplying by:

$$\frac{L}{U^2} \tag{46}$$

the equation take on the non-dimensional form that allows for dimensional analysis of the separate terms:

$$\begin{aligned}&\frac{\partial u^\star}{\partial t^\star} + u^\star\frac{\partial u^\star}{\partial x^\star} + v^\star\frac{\partial u^\star}{\partial y^\star} + w^\star\frac{\partial u^\star}{\partial z^\star} = -\frac{\partial \psi^\star}{\partial x^\star} \\ &+ \nu^\star\nu_\infty[(\frac{1}{LU})\frac{\partial^2 u^\star}{\partial {x^\star}^2} + (\frac{L}{U\delta^2})\frac{\partial^2 u^\star}{\partial {y^\star}^2} + (\frac{1}{LU})\frac{\partial^2 u^\star}{\partial {z^\star}^2}] \\ &+ (\frac{\delta}{Ut})2v^\star\omega_3^\star - (\frac{L}{Ut})2w^\star\omega_2^\star \\ &+ (\frac{L^2}{U^2t^2})x^\star[{\omega_3^\star}^2 + {\omega_2^\star}^2] \\ &- (\frac{\delta L}{U^2t^2})y^\star\omega_1^\star\omega_2^\star - (\frac{L^2}{U^2t^2})z^\star\omega_1^\star\omega_3^\star\end{aligned} \tag{47}$$

For the purposes of simplification the assumption is made that the boundary layer thickness approaches a very small number (ε^2) while the characteristic length approaches a very large number (∞):

$$\begin{aligned}\delta &\to \varepsilon^2 \\ \varepsilon &<< 1 \\ L &\to \infty\end{aligned} \tag{48}$$

At this stage not much can be said regarding the magnitude of the characteristic velocity or the time parameter. In order to keep the solution as general as possible, it will only be assumed that velocity and time has positive values:

$$\begin{aligned} \varepsilon \leq U \leq \infty \\ \varepsilon \leq t \leq \infty \end{aligned} \tag{49}$$

From the above the following simplifications can be made:

$$\begin{aligned} \frac{1}{LU} &\to \varepsilon \\ \frac{L}{\delta^2} &\to \infty \\ \frac{\delta}{L} &\to \varepsilon^2 \\ \delta L &\to \infty \end{aligned} \tag{50}$$

Implementing the above simplifications in Equation 45 leads to the general conservation of momentum for the non-inertial boundary layer equation in the x-direction:

$$\begin{aligned} \frac{\partial \hat{u}}{\partial t} + \hat{u}\frac{\partial \hat{u}}{\partial \hat{x}} + \hat{v}\frac{\partial \hat{u}}{\partial \hat{y}} + \hat{w}\frac{\partial \hat{u}}{\partial \hat{z}} &= -\frac{\partial \hat{\psi}}{\partial \hat{x}} + \nu(\frac{\partial^2 \hat{u}}{\partial \hat{y}^2}) \\ &+ 2\hat{v}\omega_3 - 2\hat{w}\omega_2 \\ &+ \hat{x}({\omega_3}^2 + {\omega_2}^2) - \hat{y}\omega_1\omega_2 - \hat{z}\omega_1\omega_3 \end{aligned} \tag{51}$$

4.3.2. Second Principle Direction Equation

The non-inertial conservation of momentum equation in the *haty*-direction is as follows:

$$\begin{aligned} \frac{\partial \hat{v}}{\partial t} + \hat{u}\frac{\partial \hat{v}}{\partial \hat{x}} + \hat{v}\frac{\partial \hat{v}}{\partial \hat{y}} + \hat{w}\frac{\partial \hat{v}}{\partial \hat{z}} &= -\frac{\partial \hat{\psi}}{\partial \hat{y}} + \nu(\frac{\partial^2 \hat{v}}{\partial \hat{x}^2} + \frac{\partial^2 \hat{v}}{\partial \hat{y}^2} + \frac{\partial^2 \hat{v}}{\partial \hat{z}^2}) \\ &+ 2\hat{w}\omega_1 - 2\hat{u}\omega_3 \\ &+ \hat{y}({\omega_3}^2 + {\omega_1}^2) - \hat{x}\omega_1\omega_2 - \hat{z}\omega_2\omega_3 \end{aligned} \tag{52}$$

Implementing the non-dimensional parameters previously defined and multiplication by:

$$\frac{\delta}{U^2} \tag{53}$$

Leads to:

$$
\begin{aligned}
&(\frac{\delta^2}{L^2})\frac{\partial v^\star}{\partial t^\star} + (\frac{\delta^2}{L^2})u^\star\frac{\partial v^\star}{\partial x^\star} + (\frac{\delta^2}{L^2})v^\star\frac{\partial v^\star}{\partial y^\star} + (\frac{\delta^2}{L^2})w^\star\frac{\partial v^\star}{\partial z^\star} \\
&= -\frac{\partial \psi^\star}{\partial y^\star} \\
&+ \nu^\star\nu_\infty((\frac{\delta^2}{UL^3})\frac{\partial^2 v^\star}{\partial x^{\star 2}} + (\frac{1}{LU})\frac{\partial^2 v^\star}{\partial y^{\star 2}} + (\frac{\delta^2}{UL^3})\frac{\partial^2 v^\star}{\partial z^{\star 2}}) \\
&+ (\frac{\delta}{Ut})2w^\star\omega_1^\star - (\frac{\delta}{Ut})2u^\star\omega_3^\star \\
&+ y^\star((\frac{\delta^2}{U^2t^2})\omega_3^{\star 2} + (\frac{\delta^2}{U^2t^2})\omega_1^{\star 2}) \\
&- (\frac{\delta L}{U^2t^2})x^\star\omega_1^\star\omega_2^\star - (\frac{\delta L}{U^2t^2})z^\star\omega_2^\star\omega_3^\star
\end{aligned}
\tag{54}
$$

When the same simplifications is used as in the $\hat{x}$-direction case, the general conservation of momentum equation for the non-inertial boundary layer equation in the $\hat{y}$-direction becomes:

$$
0 = -\frac{\partial \hat{\psi}}{\partial \hat{y}} + 2\hat{w}\omega_1 - 2\hat{u}\omega_3 + \hat{y}({\omega_3}^2 + {\omega_1}^2) - \hat{x}\omega_1\omega_2 - \hat{z}\omega_2\omega_3 \tag{55}
$$

4.3.3. Third Principle Direction Equation

The non-inertial conservation of momentum equation in the $\hat{z}$-direction is as follows:

$$
\begin{aligned}
\frac{\partial \hat{w}}{\partial t} + \hat{u}\frac{\partial \hat{w}}{\partial \hat{x}} + \hat{v}\frac{\partial \hat{w}}{\partial \hat{y}} + \hat{w}\frac{\partial \hat{w}}{\partial \hat{z}} &= -\frac{\partial \hat{\psi}}{\partial \hat{z}} + \nu(\frac{\partial^2 \hat{w}}{\partial \hat{x}^2} + \frac{\partial^2 \hat{w}}{\partial \hat{y}^2} + \frac{\partial^2 \hat{w}}{\partial \hat{z}^2}) \\
&+ 2\hat{u}\omega_2 - 2\hat{v}\omega_1 \\
&+ \hat{z}({\omega_2}^2 + {\omega_1}^2) - \hat{x}\omega_1\omega_3 - \hat{y}\omega_2\omega_3
\end{aligned}
\tag{56}
$$

Implementing the non-dimensional parameters previously defined and multiplication by:

$$
\frac{L}{U^2} \tag{57}
$$

Leads to:

$$\begin{aligned}
&\frac{\partial w^\star}{\partial t} + u^\star\frac{\partial w^\star}{\partial x^\star} + v^\star\frac{\partial w^\star}{\partial y^\star} + w^\star\frac{\partial w^\star}{\partial z^\star} = -\frac{\partial \psi^\star}{\partial z^\star} \\
&+ \nu^\star\nu_\infty[(\frac{1}{LU})\frac{\partial^2 w^\star}{\partial x^{\star 2}} + (\frac{L}{\delta U})\frac{\partial^2 w^\star}{\partial y^{\star 2}} + (\frac{1}{LU})\frac{\partial^2 w^\star}{\partial z^{\star 2}}] \\
&+ 2(\frac{L}{Ut})u^\star\omega_2 - 2(\frac{\delta}{Ut})v^\star\omega_1 \\
&+ (\frac{L^2}{U^2t^2})z^\star({\omega_2}^2 + {\omega_1}^2) \\
&- (\frac{L^2}{U^2t^2})x^\star\omega_1\omega_3 - (\frac{\delta L}{U^2t^2})y^\star\omega_2\omega_3
\end{aligned} \tag{58}$$

When the same simplifications is used as in the $\hat{x}$-direction case, the general conservation of momentum equation for the non-inertial boundary layer equation in the $\hat{z}$-direction becomes:

$$\begin{aligned}
\frac{\partial \hat{w}}{\partial t} + \hat{u}\frac{\partial \hat{w}}{\partial \hat{x}} + \hat{v}\frac{\partial \hat{w}}{\partial \hat{y}} + \hat{w}\frac{\partial \hat{w}}{\partial \hat{z}} &= -\frac{\partial \hat{\psi}}{\partial \hat{z}} + \nu(\frac{\partial^2 \hat{w}}{\partial \hat{y}^2}) \\
&+ 2\hat{u}\omega_2 - 2\hat{v}\omega_1 \\
&+ \hat{z}({\omega_2}^2 + {\omega_1}^2) - \hat{x}\omega_1\omega_3 - \hat{y}\omega_2\omega_3
\end{aligned} \tag{59}$$

4.4. Validation of Equations

In [15] the non-inertial boundary layer equations are defined as follow:

$$\begin{aligned}
u_x + u_y + u_z &= 0 \\
uu_x + vu_y + wu_z + 2\omega_2 w - \omega_r^2 r_x &= -\frac{1}{\rho}p_x + \nu u_{yy} \\
2(\omega_3 u - \omega_1 w) - \omega_r^2 r_y &= -\frac{1}{\rho}p_y \\
uw_x + vw_y + ww_z - 2\omega_2 u - \omega_r^2 r_z &= -\frac{1}{\rho}p_x + \nu w_{yy}
\end{aligned} \tag{60}$$

[15] however stated that the total change of pressure through out the boundary layer long a principle direction normal to the wall will be of $O(\delta)$ and may therefore still be neglected. The equation in the $\hat{y}$-direction can thus be simplified to:

$$-\frac{1}{\rho}p_y = 0 \tag{61}$$

The mass conservation equation for the boundary layer agrees with the equation of [15]:

$$\frac{\partial \hat{u}}{\partial \hat{x}} + \frac{\partial \hat{v}}{\partial \hat{y}} + \frac{\partial \hat{w}}{\partial \hat{z}} = 0 \tag{62}$$

The boundary layer equations derived in the previous section represents a general case where no assumptions was made with regards to the order of magnitude of characteristic velocity (U) and time (t). If it is assumed that the product of U and t is greater than one, the boundary layer equation in the x-direction will reduce to:

$$\begin{aligned} \frac{\partial \hat{u}}{\partial t} + \hat{u}\frac{\partial \hat{u}}{\partial \hat{x}} + \hat{v}\frac{\partial \hat{u}}{\partial \hat{y}} + \hat{w}\frac{\partial \hat{u}}{\partial \hat{z}} = &-\frac{\partial \hat{\psi}}{\partial \hat{x}} + \nu(\frac{\partial^2 \hat{u}}{\partial \hat{y}^2}) \\ &- 2\hat{w}\omega_2 \\ &+ \hat{x}({\omega_3}^2 + {\omega_2}^2) - \hat{y}\omega_1\omega_2 - \hat{z}\omega_1\omega_3 \end{aligned} \tag{63}$$

This equation agrees with the equation provided in [15].
Under the same assumption as above, the boundary layer in the $\hat{y}$-direction becomes:

$$0 = -\frac{\partial \hat{\psi}}{\partial \hat{y}} - \hat{x}\omega_1\omega_2 - \hat{z}\omega_2\omega_3 \tag{64}$$

If the assumption from [15], with regards to the total change of pressure through out the boundary layer long a principle direction normal to the wall, is used it is reasonable to assume the pressure is only dependant on the $\hat{x}$- and $\hat{z}$-directions and the above equation then becomes:

$$0 = -\frac{\partial \hat{\psi}}{\partial \hat{y}} \tag{65}$$

In a similar manner as explained above, the equation in the $\hat{z}$-direction will become:

$$\begin{aligned} \frac{\partial \hat{w}}{\partial t} + \hat{u}\frac{\partial \hat{w}}{\partial \hat{x}} + \hat{v}\frac{\partial \hat{w}}{\partial \hat{y}} + \hat{w}\frac{\partial \hat{w}}{\partial \hat{z}} = &-\frac{\partial \hat{\psi}}{\partial \hat{z}} + \nu(\frac{\partial^2 \hat{w}}{\partial \hat{y}^2}) \\ &+ 2\hat{u}\omega_2 \\ &+ \hat{z}({\omega_2}^2 + {\omega_1}^2) - \hat{x}\omega_1\omega_3 - \hat{y}\omega_2\omega_3 \end{aligned} \tag{66}$$

This is consistent with the equation provided in [15].

Now consider that the rotation on the flat plate is only around the $\hat{y}$-axis. In such conditions the values of the angular velocities becomes:

$$\begin{aligned} \omega_1 &= 0 \\ \omega_2 &= \Omega \\ \omega_3 &= 0 \end{aligned} \tag{67}$$

Substituting for these values in Equations 63, 65 and 66 respectively results in the following set of non-inertial boundary layer equations:

$$\begin{aligned} \frac{\partial \hat{u}}{\partial t} + \hat{u}\frac{\partial \hat{u}}{\partial \hat{x}} + \hat{v}\frac{\partial \hat{u}}{\partial \hat{y}} + \hat{w}\frac{\partial \hat{u}}{\partial \hat{z}} &= -\frac{\partial \hat{\psi}}{\partial \hat{x}} + \nu(\frac{\partial^2 \hat{u}}{\partial \hat{y}^2}) - 2\hat{w}\Omega + \hat{x}\Omega^2 \\ 0 &= -\frac{\partial \hat{\psi}}{\partial \hat{y}} \\ \frac{\partial \hat{w}}{\partial t} + \hat{u}\frac{\partial \hat{w}}{\partial \hat{x}} + \hat{v}\frac{\partial \hat{w}}{\partial \hat{y}} + \hat{w}\frac{\partial \hat{w}}{\partial \hat{z}} &= -\frac{\partial \hat{\psi}}{\partial \hat{z}} + \nu(\frac{\partial^2 \hat{w}}{\partial \hat{y}^2}) + 2\hat{u}\Omega + \hat{z}\Omega^2 \end{aligned} \tag{68}$$

This results in the same equations as in the literature for a rotating blade ([6], [7]) indicating consistency of the method. The differences in sign between the above and the cases stated in the literature is due to the difference in direction of rotation.

5. Non-Inertial Boundary Layer Equations for a Flat Plate in Rotation - Cylindrical Formulation

In some instances,such as asymptotic expansions and other analytical methods, it will be more convenient to make use of a cylindrical formulation for the boundary layer equations. Therefore the cylindrical form of the equations will now be obtained.

Consider the same plate as shown in Figure 4, but with the $\hat{x}$- and $\hat{z}$-axis written in terms of the $\hat{r}$- and $\hat{\theta}$-axis cylindrical co-ordinates. The same method of comparative orders will be used to obtain the boundary layer equations in cylindrical co-ordinates.

5.1. Non-Dimensional Parameters

The non-dimensional parameters used in this analysis is indicated below. R is the characteristic distance where, at a characteristic angle of β, the boundary layer height in the $\hat{y}$-direction is δ.

$$\begin{aligned} r^\star &= \frac{\hat{r}}{R} \\ \theta^\star &= \frac{\hat{\theta}}{\beta} \\ y^\star &= \frac{\hat{y}}{\delta} \end{aligned} \tag{69}$$

The normalized velocity components are a function of the characteristic velocity in the free stream and in the case of the velocity in the $\hat{y}$-direction, R and δ.

$$\begin{aligned} u_r^\star &= \frac{\hat{u}_r}{U_\infty} \\ u_\theta^\star &= \frac{\hat{u}_\theta}{U_\infty} \\ u_y^\star &= \frac{\hat{u}_y}{U_\infty}\frac{R}{\delta} \end{aligned} \tag{70}$$

The remainder of the parameters are normalized in the same manner as in the previous section:

$$\begin{aligned} t^\star &= t\frac{U_\infty}{R} \\ {\omega_i}^\star &= \omega_i t \\ \psi^\star &= \frac{\psi}{U_\infty^2} \\ \nu^\star &= \frac{\nu}{\nu_\infty} \end{aligned} \tag{71}$$

5.2. Continuity Equation for Boundary Layer Flows

The continuity equation in the cylindrical form is:

$$\frac{\partial \hat{u}_r}{\partial \hat{r}} + \frac{\hat{u}_r}{\hat{r}} + \frac{1}{\hat{r}}\frac{\partial \hat{u}_\theta}{\partial \hat{\theta}} + \frac{\partial \hat{u}_y}{\partial \hat{y}} = 0 \tag{72}$$

The non-dimensional form of this equation is obtained by substituting the parameters form section 5.1 into the equation:

$$\frac{\partial (u_r^\star U_\infty)}{\partial (r^\star R)} + \frac{u_r^\star U_\infty}{r^\star R} + \frac{1}{r^\star R}\frac{\partial (u_\theta^\star U_\infty)}{\partial (\theta^\star \beta)} + \frac{\partial (u_y^\star \frac{U_\infty \delta}{R})}{\partial (y^\star \delta)} = 0 \tag{73}$$

Multiplying this equation with,

$$\frac{R}{U_\infty} \tag{74}$$

Results in the non-dimensional form of the continuity equation where the order of magnitude can be used to group the terms that are of comparable order.

$$\frac{\partial u_r^\star}{\partial r^\star} + \frac{u_r^\star}{r^\star} + \frac{1}{\beta}\frac{1}{r^\star}\frac{\partial u_\theta^\star}{\partial \theta^\star} + \frac{\partial u_y^\star}{\partial y^\star} = 0 \tag{75}$$

If it is considered that β is of finite value since $0° \leqslant \beta \leqslant 360°$, and therefore of an order comparable to 1, no terms can be neglected from the equation above. The boundary layer equation for continuity there remains:

$$\frac{\partial \hat{u}_r}{\partial \hat{r}} + \frac{\hat{u}_r}{\hat{r}} + \frac{1}{\hat{r}}\frac{\partial \hat{u}_\theta}{\partial \hat{\theta}} + \frac{\partial \hat{u}_y}{\partial \hat{y}} = 0 \tag{76}$$

5.3. Conservation of Momentum Equation for Boundary Layer Flows

The vector form of non-inertial conservation of momentum equation is derived in Appendix A and shown in Equation 15. The component form of this equation can either be expressed in Cartesian co-ordinates (Equations 45, 52 and 56) or in cylindrical co-ordinates as indicted in the next section.

5.3.1. First Principle Direction Equation

The component form of the non-inertial momentum equation in the first principle direction (in this case taken as the $\hat{r}$-direction) is indicated below:

$$\begin{aligned}\frac{\partial \hat{u}_r}{\partial t} + \hat{u}_r\frac{\partial \hat{u}_r}{\partial \hat{r}} + \frac{\hat{u}_\theta}{\hat{r}}\frac{\partial \hat{u}_r}{\partial \hat{\theta}} - \frac{\hat{u}_\theta^2}{\hat{r}} + \hat{u}_y\frac{\partial \hat{u}_r}{\partial \hat{y}} &= -\frac{\partial \hat{\psi}}{\partial \hat{r}} \\ &+ \hat{\nu}\Big[\frac{\partial^2 \hat{u}_r}{\partial \hat{r}^2} + \frac{1}{\hat{r}}\frac{\partial \hat{u}_r}{\partial \hat{r}} + \frac{1}{\hat{r}^2}\frac{\partial^2 \hat{u}_r}{\partial \hat{\theta}^2} - \frac{2}{\hat{r}^2}\frac{\partial \hat{u}_\theta}{\partial \hat{\theta}} - \frac{\hat{u}_r}{\hat{r}^2} + \frac{\partial^2 \hat{u}_r}{\partial \hat{y}^2}\Big] \\ &\underbrace{-2\hat{u}_\theta\omega_y + 2\hat{u}_y\omega_\theta}_{\text{Coriolis}} \underbrace{- \hat{y}\omega_r\omega_y + \hat{r}\omega_y^2 + \hat{r}\omega_\theta^2}_{\text{Centrifugal}}\end{aligned} \tag{77}$$

Substitution of the non-dimensional parameters, as defined in *Section 5.1* , into the equation, results in the non-dimensional form of the equation:

$$\begin{aligned}\Big[\frac{U_\infty^2}{R}\Big]\frac{\partial u_r^\star}{\partial t^\star} + \Big[\frac{U_\infty^2}{R}\Big]u_r^\star\frac{\partial u_r^\star}{\partial r^\star} + \Big[\frac{U_\infty^2}{R\beta}\Big]\frac{u_\theta^\star}{r^\star}\frac{\partial u_r^\star}{\partial \theta^\star} - \Big[\frac{U_\infty^2}{R}\Big]\frac{u_\theta^{\star 2}}{r^\star} + \Big[\frac{U_\infty^2}{R}\Big]u_y^\star\frac{\partial u_r^\star}{\partial y^\star} = \\ - \Big[\frac{U_\infty^2}{R}\Big]\frac{\partial \psi^\star}{\partial r^\star} + \Big[\frac{U_\infty}{R^2}\Big]\nu^\star\nu_\infty\frac{\partial^2 u_r^\star}{\partial r^{\star 2}} + \Big[\frac{U_\infty}{R^2}\Big]\nu^\star\nu_\infty\frac{1}{r^\star}\frac{\partial u_r^\star}{\partial r^\star} \\ + \Big[\frac{U_\infty}{R^2\beta^2}\Big]\nu^\star\nu_\infty\frac{1}{r^{\star 2}}\frac{\partial^2 u_r^\star}{\partial \theta^{\star 2}} - \Big[\frac{U_\infty}{R^2\beta}\Big]\nu^\star\nu_\infty\frac{2}{r^{\star 2}}\frac{\partial u_\theta^\star}{\partial \theta^\star} - \Big[\frac{U_\infty}{R^2}\Big]\nu^\star\nu_\infty\frac{u_r^\star}{r^{\star 2}} \\ + \Big[\frac{U_\infty}{\delta^2}\Big]\nu^\star\nu_\infty\frac{\partial^2 u_r^\star}{\partial y^{\star 2}} - \Big[\frac{U_\infty}{t}\Big]2u_\theta^\star\omega_y^\star + \Big[\frac{U_\infty\delta}{Rt}\Big]2u_y^\star\omega_\theta^\star - \Big[\frac{\delta}{t^2}\Big]y^\star\omega_r^\star\omega_y^\star \\ + \Big[\frac{R}{t^2}\Big]r^\star\omega_y^{\star 2} + \Big[\frac{R}{t^2}\Big]r^\star\omega_\theta^{\star 2}\end{aligned} \tag{78}$$

Multiplying the equation above with,

$$\frac{R}{U_\infty^2} \tag{79}$$

Results in a non-dimensional form where the order of magnitude of the terms can be evaluated:

$$\begin{aligned}\frac{\partial u_r^\star}{\partial t^\star} + u_r^\star\frac{\partial u_r^\star}{\partial r^\star} + \Big[\frac{1}{\beta}\Big]\frac{u_\theta^\star}{r^\star}\frac{\partial u_r^\star}{\partial \theta^\star} - \frac{u_\theta^{\star 2}}{r^\star} + u_y^\star\frac{\partial u_r^\star}{\partial y^\star} = -\frac{\partial \psi^\star}{\partial r^\star} + \Big[\frac{1}{U_\infty R}\Big]\nu^\star\nu_\infty\frac{\partial^2 u_r^\star}{\partial r^{\star 2}} \\ + \Big[\frac{1}{U_\infty R}\Big]\nu^\star\nu_\infty\frac{1}{r^\star}\frac{\partial u_r^\star}{\partial r^\star} + \Big[\frac{1}{U_\infty R\beta^2}\Big]\nu^\star\nu_\infty\frac{1}{r^{\star 2}}\frac{\partial^2 u_r^\star}{\partial \theta^{\star 2}} - \Big[\frac{1}{U_\infty R\beta}\Big]\nu^\star\nu_\infty\frac{2}{r^{\star 2}}\frac{\partial u_\theta^\star}{\partial \theta^\star} \\ - \Big[\frac{1}{U_\infty R}\Big]\nu^\star\nu_\infty\frac{u_r^\star}{r^{\star 2}} + \Big[\frac{R}{U_\infty\delta^2}\Big]\nu^\star\nu_\infty\frac{\partial^2 u_r^\star}{\partial y^{\star 2}} - \Big[\frac{R}{U_\infty t}\Big]2u_\theta^\star\omega_y^\star + \Big[\frac{\delta}{U_\infty t}\Big]2u_y^\star\omega_\theta^\star \\ - \Big[\frac{\delta R}{U_\infty^2 t^2}\Big]y^\star\omega_r^\star\omega_y^\star + \Big[\frac{R^2}{U_\infty^2 t^2}\Big]r^\star\omega_y^{\star 2} + \Big[\frac{R^2}{U_\infty^2 t^2}\Big]r^\star\omega_\theta^{\star 2}\end{aligned} \tag{80}$$

As was done previously for the purposes of simplification, the assumption is made that the boundary layer thickness approaches a very small number (ε^2)

while the characteristic length approaches a very large number (∞):

$$\begin{aligned} \delta &\to \varepsilon^2 \\ \varepsilon &<< 1 \\ R &\to \infty \end{aligned} \tag{81}$$

In order to keep the solution as general as possible, it will be assumed that velocity, time and characteristic angle has positive values:

$$\begin{aligned} \varepsilon \leq U_\infty \leq \infty \\ \varepsilon \leq t \leq \infty \\ 0^\circ \leqslant \beta \leqslant 360^\circ \end{aligned} \tag{82}$$

From the above the following simplifications can be made:

$$\begin{aligned} \frac{1}{U_\infty R} &\to \varepsilon \\ \frac{R}{\delta^2} &\to \infty \\ \delta R &\to \infty \end{aligned} \tag{83}$$

Following from the above, the most general form of the $\hat{r}$-momentum boundary layer equation becomes:

$$\begin{aligned} \frac{\partial \hat{u}_r}{\partial t} + \hat{u}_r \frac{\partial \hat{u}_r}{\partial \hat{r}} + \frac{\hat{u}_\theta}{\hat{r}} \frac{\partial \hat{u}_r}{\partial \hat{\theta}} - \frac{\hat{u}_\theta^2}{\hat{r}} + \hat{u}_y \frac{\partial \hat{u}_r}{\partial \hat{y}} = -\frac{\partial \hat{\psi}}{\partial \hat{r}} + \hat{\nu} \frac{\partial^2 \hat{u}_r}{\partial \hat{y}^2} - 2\hat{u}_\theta \omega_y + 2\hat{u}_y \omega_\theta \\ - \hat{y}\omega_r \omega_y + \hat{r}\omega_y^2 + \hat{r}\omega_\theta^2 \end{aligned} \tag{84}$$

5.3.2. Second Principle Direction Equation

The components form of the momentum equation in the $\hat{\theta}$-direction is expressed as:

$$\begin{aligned} \frac{\partial \hat{u}_\theta}{\partial t} + \hat{u}_r \frac{\partial \hat{u}_\theta}{\partial \hat{r}} + \frac{\hat{u}_\theta}{\hat{r}} \frac{\partial \hat{u}_\theta}{\partial \hat{\theta}} + \frac{\hat{u}_\theta \hat{u}_r}{\hat{r}} + \hat{u}_y \frac{\partial \hat{u}_\theta}{\partial \hat{y}} = -\frac{1}{\hat{r}} \frac{\partial \hat{\psi}}{\partial \hat{\theta}} \\ + \hat{\nu} \Big[\frac{\partial^2 \hat{u}_\theta}{\partial \hat{r}^2} + \frac{1}{\hat{r}} \frac{\partial \hat{u}_\theta}{\partial \hat{r}} + \frac{1}{\hat{r}^2} \frac{\partial^2 \hat{u}_\theta}{\partial \hat{\theta}^2} - \frac{2}{\hat{r}^2} \frac{\partial \hat{u}_r}{\partial \hat{\theta}} - \frac{\hat{u}_\theta}{\hat{r}^2} + \frac{\partial^2 \hat{u}_\theta}{\partial \hat{y}^2} \Big] \\ \underbrace{-2\hat{u}_y \omega_r + 2\hat{u}_r \omega_y}_{\text{Coriolis}} \underbrace{- \hat{r}\omega_r \omega_\theta - \hat{y}\omega_\theta \omega_r}_{\text{Centrifugal}} \end{aligned} \tag{85}$$

Substituting the non-dimensional parameters of *Section 5.1* into the equation above yields:

$$\begin{aligned}\Big[\frac{U_\infty^2}{R}\Big]\frac{\partial u_\theta^\star}{\partial t^\star}+\Big[\frac{U_\infty^2}{R}\Big]u_r^\star\frac{\partial u_\theta^\star}{\partial r^\star}+\Big[\frac{U_\infty^2}{\beta R}\Big]\frac{u_\theta^\star}{r^\star}\frac{\partial u_\theta^\star}{\partial\theta^\star}+\Big[\frac{U_\infty^2}{R}\Big]\frac{u_\theta^\star u_r^\star}{r^\star}+\Big[\frac{U_\infty^2}{R}\Big]u_y^\star\frac{\partial u_\theta^\star}{\partial y^\star}=\\ -\Big[\frac{U_\infty^2}{\beta R}\Big]\frac{1}{r^\star}\frac{\partial\psi^\star}{\partial\theta^\star}+\Big[\frac{U_\infty}{R^2}\Big]\nu^\star\nu_\infty\frac{\partial^2 u_\theta^\star}{\partial r^{\star 2}}+\Big[\frac{U_\infty}{R^2}\Big]\nu^\star\nu_\infty\frac{1}{r^\star}\frac{\partial u_\theta^\star}{\partial r^\star}\\ +\Big[\frac{U_\infty}{\beta^2R^2}\Big]\nu^\star\nu_\infty\frac{1}{r^{\star 2}}\frac{\partial^2 u_\theta^\star}{\partial\theta^{\star 2}}-\Big[\frac{U_\infty}{\beta^2R^2}\Big]\nu^\star\nu_\infty\frac{2}{r^{\star 2}}\frac{\partial u_r^\star}{\partial\theta^\star}-\Big[\frac{U_\infty}{R^2}\Big]\nu^\star\nu_\infty\frac{u_\theta^\star}{r^{\star 2}}\\ +\Big[\frac{U_\infty}{\delta^2}\Big]\nu^\star\nu_\infty\frac{\partial^2 u_\theta^\star}{\partial y^{\star 2}}+\Big[\frac{U_\infty\delta}{Rt}\Big]2u_y^\star\omega_r^\star-\Big[\frac{U_\infty}{t}\Big]2u_r^\star\omega_y^\star\\ -\Big[\frac{R}{t^2}\Big]r^\star\omega_r^\star\omega_\theta^\star-\Big[\frac{\delta}{t^2}\Big]y^\star\omega_\theta^\star\omega_r^\star\end{aligned}\tag{86}$$

Multiplying the equation above with,

$$\frac{\beta R}{U_\infty^2}\tag{87}$$

Results in the non-dimensional form of the $\hat{\theta}$-momentum equation.

$$\begin{aligned}\beta\frac{\partial u_\theta^\star}{\partial t^\star}+\beta u_r^\star\frac{\partial u_\theta^\star}{\partial r^\star}+\frac{u_\theta^\star}{r^\star}\frac{\partial u_\theta^\star}{\partial\theta^\star}+\beta\frac{u_\theta^\star u_r^\star}{r^\star}+\beta u_y^\star\frac{\partial u_\theta^\star}{\partial y^\star}=-\frac{1}{r^\star}\frac{\partial\psi^\star}{\partial\theta^\star}\\ +\Big[\frac{\beta}{U_\infty R}\Big]\nu^\star\nu_\infty\frac{\partial^2 u_\theta^\star}{\partial r^{\star 2}}+\Big[\frac{\beta}{U_\infty R}\Big]\nu^\star\nu_\infty\frac{1}{r^\star}\frac{\partial u_\theta^\star}{\partial r^\star}+\Big[\frac{1}{U_\infty R\beta}\Big]\nu^\star\nu_\infty\frac{1}{r^{\star 2}}\frac{\partial^2 u_\theta^\star}{\partial\theta^{\star 2}}\\ -\Big[\frac{1}{U_\infty R\beta}\Big]\nu^\star\nu_\infty\frac{2}{r^{\star 2}}\frac{\partial u_r^\star}{\partial\theta^\star}-\Big[\frac{\beta}{U_\infty R}\Big]\nu^\star\nu_\infty\frac{u_\theta^\star}{r^{\star 2}}+\Big[\frac{\beta R}{U_\infty\delta^2}\Big]\nu^\star\nu_\infty\frac{\partial^2 u_\theta^\star}{\partial y^{\star 2}}\\ +\Big[\frac{\beta\delta}{U_\infty t}\Big]2u_y^\star\omega_r^\star-\Big[\frac{\beta R}{U_\infty t}\Big]2u_r^\star\omega_y^\star-\Big[\frac{\beta R^2}{U_\infty^2t^2}\Big]r^\star\omega_r^\star\omega_\theta^\star-\Big[\frac{\beta\delta R}{U_\infty^2t^2}\Big]y^\star\omega_\theta^\star\omega_r^\star\end{aligned}\tag{88}$$

The same simplifications that was done for the $\hat{r}$-momentum equation is employed here to obtain the $\hat{\theta}$-momentum equation:

$$\begin{aligned}\frac{\partial\hat{u}_\theta}{\partial t}+\hat{u}_r\frac{\partial\hat{u}_\theta}{\partial\hat{r}}+\frac{\hat{u}_\theta}{\hat{r}}\frac{\partial\hat{u}_\theta}{\partial\hat{\theta}}+\frac{\hat{u}_\theta\hat{u}_r}{\hat{r}}+\hat{u}_y\frac{\partial\hat{u}_\theta}{\partial\hat{y}}=-\frac{1}{\hat{r}}\frac{\partial\hat{\psi}}{\partial\hat{\theta}}+\hat{\nu}\frac{\partial^2\hat{u}_\theta}{\partial\hat{y}^2}+2\hat{u}_y\omega_r-2\hat{u}_r\omega_y\\ -\hat{r}\omega_r\omega_\theta-\hat{y}\omega_\theta\omega_r\end{aligned}\tag{89}$$

5.3.3. Third Principle Direction Equation

The component form of the conservation of momentum equation in the $\hat{y}$-direction is expressed as follow:

$$\begin{aligned}\frac{\partial\hat{u}_y}{\partial t}+\hat{u}_r\frac{\partial\hat{u}_y}{\partial\hat{r}}+\frac{\hat{u}_\theta}{\hat{r}}\frac{\partial\hat{u}_y}{\partial\hat{\theta}}+\hat{u}_y\frac{\partial\hat{u}_y}{\partial\hat{y}}=-\frac{\partial\hat{\psi}}{\partial\hat{y}}+\nu\Big[\frac{\partial^2\hat{u}_y}{\partial\hat{r}^2}+\frac{1}{\hat{r}}\frac{\partial\hat{u}_y}{\partial\hat{r}}+\frac{1}{\hat{r}^2}\frac{\partial^2\hat{u}_y}{\partial\hat{\theta}^2}+\frac{\partial^2\hat{u}_y}{\partial\hat{y}^2}\Big]\\ \underbrace{+2\hat{u}_r\omega_\theta-2\hat{u}_\theta\omega_r}_{\text{Coriolis}}\underbrace{-\hat{r}\omega_r\omega_y+\hat{y}\omega_r^2+\hat{y}\omega_\theta^2}_{\text{Centrifugal}}\end{aligned}\tag{90}$$

Substitution of the equations as shown in *Section 5.1* will result in the expression:

$$\begin{aligned}\Big[\frac{U_\infty^2\delta}{R^2}\Big]\frac{\partial u_y^\star}{\partial t^\star}+\Big[\frac{U_\infty^2\delta}{R^2}\Big]u_r^\star\frac{\partial u_y^\star}{\partial r^\star}+\Big[\frac{U_\infty^2}{R^2}\Big]\frac{u_\theta^\star}{r^\star}\frac{\partial u_y^\star}{\partial\theta^\star}+\Big[\frac{U_\infty^2\delta}{R^2}\Big]u_y^\star\frac{\partial u_y^\star}{\partial y^\star}=-\Big[\frac{U_\infty^2}{\delta}\Big]\frac{\partial\psi^\star}{\partial y^\star}\\+\Big[\frac{U_\infty\delta}{R^3}\Big]\nu^\star\nu_\infty\frac{\partial^2 u_y^\star}{\partial r^{\star\,2}}+\Big[\frac{U_\infty\delta}{R^3}\Big]\nu^\star\nu_\infty\frac{1}{r^\star}\frac{\partial u_y^\star}{\partial r^\star}+\Big[\frac{U_\infty\delta}{\beta^2R^3}\Big]\nu^\star\nu_\infty\frac{1}{r^{\star\,2}}\frac{\partial^2 u_y^\star}{\partial\theta^{\star\,2}}\\+\Big[\frac{U_\infty}{\delta R}\Big]\nu^\star\nu_\infty\frac{\partial^2 u_y^\star}{\partial y^{\star\,2}}+\Big[\frac{U_\infty}{t}\Big]2u_r^\star\omega_\theta^\star-\Big[\frac{U_\infty}{t}\Big]2u_\theta^\star\omega_r^\star-\Big[\frac{R}{t^2}\Big]r^\star\omega_r^\star\omega_y^\star\\+\Big[\frac{\delta}{t^2}\Big]y^\star\omega_r^{\star\,2}+\Big[\frac{\delta}{t^2}\Big]y^\star\omega_\theta^{\star\,2}\end{aligned}\tag{91}$$

Multiply the equation above with,

$$\frac{\delta}{U_\infty^2}\tag{92}$$

results in the non-dimensional form of the equation:

$$\begin{aligned}\Big[\frac{\delta^2}{R^2}\Big]\frac{\partial u_y^\star}{\partial t^\star}+\Big[\frac{\delta^2}{R^2}\Big]u_r^\star\frac{\partial u_y^\star}{\partial r^\star}+\Big[\frac{\delta}{R^2}\Big]\frac{u_\theta^\star}{r^\star}\frac{\partial u_y^\star}{\partial\theta^\star}+\Big[\frac{\delta^2}{R^2}\Big]u_y^\star\frac{\partial u_y^\star}{\partial y^\star}=-\frac{\partial\psi^\star}{\partial y^\star}\\+\Big[\frac{\delta^2}{U_\infty R^3}\Big]\nu^\star\nu_\infty\frac{\partial^2 u_y^\star}{\partial r^{\star\,2}}+\Big[\frac{\delta^2}{U_\infty R^3}\Big]\nu^\star\nu_\infty\frac{1}{r^\star}\frac{\partial u_y^\star}{\partial r^\star}\\+\Big[\frac{\delta^2}{U_\infty\beta^2R^3}\Big]\nu^\star\nu_\infty\frac{1}{r^{\star\,2}}\frac{\partial^2 u_y^\star}{\partial\theta^{\star\,2}}+\Big[\frac{1}{U_\infty R}\Big]\nu^\star\nu_\infty\frac{\partial^2 u_y^\star}{\partial y^{\star\,2}}+\Big[\frac{\delta}{U_\infty t}\Big]2u_r^\star\omega_\theta^\star\\-\Big[\frac{\delta}{U_\infty t}\Big]2u_\theta^\star\omega_r^\star-\Big[\frac{R\delta}{U_\infty^2t^2}\Big]r^\star\omega_r^\star\omega_y^\star+\Big[\frac{\delta^2}{U_\infty^2t^2}\Big]y^\star\omega_r^{\star\,2}+\Big[\frac{\delta^2}{U_\infty^2t^2}\Big]y^\star\omega_\theta^{\star\,2}\end{aligned}\tag{93}$$

The simplification assumptions that was made in *Section 5.3.1* is used here to arrive at the boundary layer equation in the $\hat{y}$-direction for cylindrical co-ordinates:

$$0=-\frac{\partial\hat{\psi}}{\partial\hat{y}}+2\hat{u}_r\omega_\theta-2\hat{u}_\theta\omega_r-\hat{r}\omega_r\omega_y+\hat{y}\omega_r^2+\hat{y}\omega_\theta^2\tag{94}$$

5.4. Validation of Equations

The cylindrical form of the Navier-Stokes equations can be expressed, as in the Cartesian case, in the inertial or the non-inertial form. Expressing a set of equations, that was originally in the Cartesian system, in cylindrical co-ordinates does not place it in the non-inertial frame. This misconception was noted in [16] as shown in Equation 95 where certain cylindrical terms (as marked in the equation) where described as the Centrifugal and Coriolis forces

respectively. Those terms are merely part of the material derivative in the cylindrical system and has bears no relevance to the fictitious forces. This will we shown in the sections below.

$$\begin{aligned}\frac{\partial u_r}{\partial t}+u_r\frac{\partial u_r}{\partial r}+\frac{u_\theta}{r}\frac{\partial u_r}{\partial \theta}-\overbrace{\frac{u_\theta^2}{r}}^{\cancel{\text{Centrifugal}}}+u_y\frac{\partial u_r}{\partial y}&=-\frac{\partial \psi}{\partial r}\\ +\nu\Big[\frac{\partial^2 u_r}{\partial r^2}+\frac{1}{r}\frac{\partial u_r}{\partial r}+\frac{1}{r^2}\frac{\partial^2 u_r}{\partial \theta^2}-\frac{2}{r^2}\frac{\partial u_\theta}{\partial \theta}-\frac{u_r}{r^2}+\frac{\partial^2 u_r}{\partial y^2}\Big]&\end{aligned} \tag{95}$$

$$\begin{aligned}\frac{\partial u_\theta}{\partial t}+u_r\frac{\partial u_\theta}{\partial r}+\frac{u_\theta}{r}\frac{\partial u_\theta}{\partial \theta}+\overbrace{\frac{u_\theta u_r}{r}}^{\cancel{\text{Coriolis}}}+u_y\frac{\partial u_\theta}{\partial y}&=-\frac{1}{r}\frac{\partial \psi}{\partial \theta}\\ +\nu\Big[\frac{\partial^2 u_\theta}{\partial r^2}+\frac{1}{r}\frac{\partial u_\theta}{\partial r}+\frac{1}{r^2}\frac{\partial^2 u_\theta}{\partial \theta^2}-\frac{2}{r^2}\frac{\partial u_r}{\partial \theta}-\frac{u_\theta}{r^2}+\frac{\partial^2 u_\theta}{\partial y^2}\Big]&\end{aligned}$$

The cylindrical system is just an alternative way of describing the motion (see Figure 5) and has, as in the Cartesian formulation, different forms in the inertial and non-inertial frames. The vector form of the non-inertial Navier-Stokes equations are independent from co-ordinates system. The differences in the system of equations (Cartesian and Cylindrical), only becomes apparent when written in component form.

Figure 5: Cartesian vs Cylindrical descriptions of point P

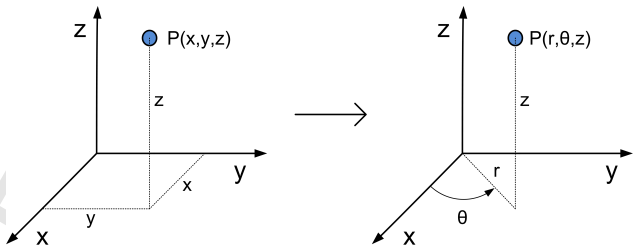

Validation of the equations in *Sections 5.2 and 5.3* will be done by converting Equations 44, 51, 55, 59 to the cylindrical system. This should result in a set of equations that is exactly the same as Equations 76, 84, 94, 89.

5.4.1. Conversion

The Cartesian positions is related to the Cylindrical positions as shown below where it will be assumed that the $\hat{y}$-axis remains common between the co-ordinates systems:

$$\begin{aligned} \hat{x} &= \hat{r}cos\hat{\theta} \\ \hat{y} &= \hat{y} \\ \hat{z} &= \hat{r}sin\hat{\theta} \end{aligned} \tag{96}$$

The velocity components is therefore related by:

$$\begin{aligned} \hat{u} &= \hat{u}_r cos\hat{\theta} - \hat{u}_\theta sin\hat{\theta} \\ \hat{v} &= \hat{u}_y \\ \hat{w} &= \hat{u}_r sin\hat{\theta} + \hat{u}_\theta cos\hat{\theta} \end{aligned} \tag{97}$$

The derivatives of one system are converted by means of the matrix:

$$\begin{bmatrix} \frac{\partial\hat{\phi}}{\partial\hat{x}} \\ \frac{\partial\hat{\phi}}{\partial\hat{y}} \\ \frac{\partial\hat{\phi}}{\partial\hat{z}v} \end{bmatrix} = \begin{bmatrix} \cos\hat{\theta} & -\frac{sin\hat{\theta}}{\hat{r}} & 0 \\ 0 & 0 & 1 \\ \sin\hat{\theta} & \frac{cos\hat{\theta}}{\hat{r}} & 0 \end{bmatrix} \begin{bmatrix} \frac{\partial\hat{\phi}}{\partial\hat{r}} \\ \frac{\partial\hat{\phi}}{\partial\hat{\theta}} \\ \frac{\partial\hat{\phi}}{\partial\hat{y}} \end{bmatrix} \tag{98}$$

The relations above will be used to convert between the co-ordinates systems in the section below to obtain the non-inertial boundary layer equations.

5.4.2. Continuity

The continuity equation for the boundary layer was derived in *Section 4.2* en resulted in Equation 44:

$$\frac{\partial\hat{u}}{\partial\hat{x}} + \frac{\partial\hat{v}}{\partial\hat{y}} + \frac{\partial\hat{w}}{\partial\hat{z}} = 0 \tag{99}$$

Substitution with the equations as shown in the previous section, and re-ordering of the terms, leads to the following expressions:

$$\begin{aligned} \big(cos\hat{\theta}\frac{\partial}{\partial\hat{r}} - \frac{sin\hat{\theta}}{\hat{r}}\frac{\partial}{\partial\hat{\theta}}\big)(\hat{u}_r cos\hat{\theta} - \hat{u}_\theta sin\hat{\theta}) + \big(sin\hat{\theta}\frac{\partial}{\partial\hat{r}} + \frac{cos\hat{\theta}}{\hat{r}}\frac{\partial}{\partial\hat{\theta}}\big)(\hat{u}_r sin\hat{\theta} + \hat{u}_\theta cos\hat{\theta}) \\ + \frac{\partial\hat{u}_y}{\partial\hat{y}} = 0 \\ \frac{\partial\hat{u}_r}{\partial\hat{r}}\big(cos^2\hat{\theta} + sin^2\hat{\theta}\big) + \frac{\hat{u}_r}{\hat{r}}\big(cos^2\hat{\theta} + sin^2\hat{\theta}\big) + \frac{1}{\hat{r}}\frac{\partial\hat{u}_\theta}{\partial\hat{\theta}}\big(cos^2\hat{\theta} + sin^2\hat{\theta}\big) + \frac{\partial\hat{u}_y}{\partial\hat{y}} = 0 \end{aligned} \tag{100}$$

When the identity,

$$cos^2\hat{\theta} + sin^2\hat{\theta} = 1 \tag{101}$$

is considered, the final equation becomes:

$$\frac{\partial \hat{u}_r}{\partial \hat{r}} + \frac{\hat{u}_r}{\hat{r}} + \frac{1}{\hat{r}}\frac{\partial \hat{u}_\theta}{\partial \hat{\theta}} + \frac{\partial \hat{u}_z}{\partial \hat{z}} = 0 \tag{102}$$

This is the equation for the boundary layer in cylindrical coordinates and is te same as Equation 76 derived in *Section 4.2*

5.4.3. Momentum Equations

The non-inertial $\hat{x}$-momentum equation, as derived in *Section 4.3* Equation 51, is:

$$\begin{aligned}\frac{\partial \hat{u}}{\partial t} + \hat{u}\frac{\partial \hat{u}}{\partial \hat{x}} + \hat{v}\frac{\partial \hat{u}}{\partial \hat{y}} + \hat{w}\frac{\partial \hat{u}}{\partial \hat{z}} = -\frac{\partial \hat{\psi}}{\partial \hat{x}} + \nu(\frac{\partial^2 \hat{u}}{\partial \hat{y}^2}) + 2\hat{v}\omega_3 - 2\hat{w}\omega_2 \\ + \hat{x}({\omega_3}^2 + {\omega_2}^2) - \hat{y}\omega_1\omega_2 - \hat{z}\omega_1\omega_3\end{aligned} \tag{103}$$

This can be converted to the Cylindrical co-ordinates system piece by piece to result in the final equation.

The transient term, with substitution of the conversions indicated in *Section 5.4.1* can be expanded to the following:

$$\begin{aligned}\frac{\partial \hat{u}}{\partial t} &\rightarrow \frac{\partial}{\partial t}(\hat{u}_r cos\hat{\theta} - \hat{u}_\theta sin\hat{\theta}) \\ \frac{\partial}{\partial t}(\hat{u}_r cos\hat{\theta} - \hat{u}_\theta sin\hat{\theta}) &= \frac{\partial \hat{u}_r}{\partial t}cos\hat{\theta} + \frac{\partial cos\hat{\theta}}{\partial t}\hat{u}_r - \frac{\partial \hat{u}_\theta}{\partial t}sin\hat{\theta} - \frac{\partial sin\hat{\theta}}{\partial t}\hat{u}_\theta\end{aligned} \tag{104}$$

If it is assumed that $\hat{\theta} \rightarrow \varepsilon$ where $\varepsilon \rightarrow 0$, then $cos\hat{\theta} \rightarrow 1$ and $sin\hat{\theta} \rightarrow 0$. The equation above will then simplify to:

$$\frac{\partial \hat{u}}{\partial t} \rightarrow \frac{\partial \hat{u}_r}{\partial t} \tag{105}$$

The remainder of the terms is converted in a similar manner:

$$
\begin{aligned}
&\text{Advection terms}\\
&\hat{u}\frac{\partial \hat{u}}{\partial \hat{x}} \rightarrow \hat{u}_r\frac{\partial \hat{u}_r}{\partial \hat{r}}\\
&\hat{v}\frac{\partial \hat{u}}{\partial \hat{y}} \rightarrow \hat{u}_y\frac{\partial \hat{u}_r}{\partial \hat{y}}\\
&\hat{w}\frac{\partial \hat{u}}{\partial \hat{z}} \rightarrow \frac{\hat{u}_\theta}{\hat{r}}\frac{\partial \hat{u}_r}{\partial \hat{\theta}} - \frac{\hat{u}_\theta^2}{\hat{r}}\\
&\text{Pressure term,}\\
&\frac{\partial \hat{\psi}}{\partial \hat{x}} \rightarrow \frac{\partial \hat{\psi}}{\partial \hat{r}}\\
&\text{Diffusion term,}\\
&\frac{\partial^2 \hat{u}}{\partial \hat{y}^2} \rightarrow \frac{\partial^2 \hat{u}_r}{\partial \hat{y}^2}\\
&\text{Coriolis terms,}\\
&2\hat{v}\hat{\omega}_3 - 2\hat{w}\hat{\omega}_2 \rightarrow [2\hat{u}_y(\hat{\omega}_r sin\hat{\theta} + \hat{\omega}_\theta cos\hat{\theta}) - 2(\hat{u}_r sin\hat{\theta} + u_{\hat{\theta}} cos\hat{\theta})\hat{\omega}_z]\\
&\rightarrow 2\hat{u}_y\omega_\theta - 2\hat{u}_\theta\omega_y\\
&\text{Centrifugal terms,}\\
&\hat{x}(\hat{\omega}_3^2 + \hat{\omega}_2^2) - \hat{y}\hat{\omega}_1\hat{\omega}_2 - \hat{z}\hat{\omega}_1\hat{\omega}_3 \rightarrow -\hat{y}\hat{\omega}_r\hat{\omega}_y + \hat{r}\hat{\omega}_y^2 + \hat{r}\hat{\omega}_\theta^2
\end{aligned}
\tag{106}
$$

This conversion will lead to the non-inertial form of the $\hat{r}$-momentum, which is the same as as the derived Equation 84:

$$
\begin{aligned}
\frac{\partial \hat{u}_r}{\partial t} + \hat{u}_r\frac{\partial \hat{u}_r}{\partial \hat{r}} + \frac{\hat{u}_\theta}{\hat{r}}\frac{\partial \hat{u}_r}{\partial \hat{\theta}} - \frac{\hat{u}_\theta^2}{\hat{r}} + \hat{u}_y\frac{\partial \hat{u}_r}{\partial \hat{y}} = &-\frac{\partial \hat{\psi}}{\partial \hat{r}} + \hat{\nu}\frac{\partial^2 \hat{u}_r}{\partial \hat{y}^2} - 2\hat{u}_\theta\omega_y + 2\hat{u}_y\omega_\theta\\
&- \hat{y}\omega_r\omega_y + \hat{r}\omega_y^2 + \hat{r}\omega_\theta^2
\end{aligned}
\tag{107}
$$

In a similar manner similarly the conversion of Equations 55 and 59 will lead to equations that is the same as the derived Equations 89 and 94 respectively.

$\hat{\theta}$-momentum

$$
\begin{aligned}
&\frac{\partial \hat{u}_\theta}{\partial t} + \hat{u}_r\frac{\partial \hat{u}_\theta}{\partial \hat{r}} + \frac{\hat{u}_\theta}{\hat{r}}\frac{\partial \hat{u}_\theta}{\partial \hat{\theta}} + \frac{\hat{u}_\theta\hat{u}_r}{\hat{r}} + \hat{u}_y\frac{\partial \hat{u}_\theta}{\partial \hat{y}} = -\frac{1}{\hat{r}}\frac{\partial \hat{\psi}}{\partial \hat{\theta}} + \hat{\nu}\frac{\partial^2 \hat{u}_\theta}{\partial \hat{y}^2} + 2\hat{u}_y\hat{\omega}_r\\
&- 2\hat{u}_r\hat{\omega}_y - \hat{r}\hat{\omega}_r\hat{\omega}_\theta - \hat{y}\hat{\omega}_\theta\hat{\omega}_r\\
&0 = -\frac{\partial \hat{\psi}}{\partial \hat{y}} + 2\hat{u}_r\hat{\omega}_\theta - 2\hat{u}_\theta\hat{\omega}_r - \hat{r}\hat{\omega}_r\hat{\omega}_y + \hat{y}\hat{\omega}_r^2 + \hat{y}\hat{\omega}_\theta^2
\end{aligned}
\tag{108}
$$

Implementing the same conditions as in Equation 67 where rotation about

the $\hat{y}$-axis was considered,

$$\begin{aligned} \hat{\omega}_r &= 0 \\ \hat{\omega}_\theta &= 0 \\ \hat{\omega}_y &= \Omega \end{aligned} \tag{109}$$

results in the following set of non-inertial boundary layer equations:

$$\begin{aligned} \frac{\partial \hat{u}_r}{\partial t} + \hat{u}_r \frac{\partial \hat{u}_r}{\partial \hat{r}} + \frac{\hat{u}_\theta}{\hat{r}} \frac{\partial \hat{u}_r}{\partial \hat{\theta}} - \frac{\hat{u}_\theta^2}{\hat{r}} + \hat{u}_y \frac{\partial \hat{u}_r}{\partial \hat{y}} &= -\frac{\partial \hat{\psi}}{\partial \hat{r}} + \hat{\nu} \frac{\partial^2 \hat{u}_r}{\partial \hat{y}^2} - 2\hat{u}_\theta \Omega + \hat{r}\Omega^2 \\ \frac{\partial \hat{u}_\theta}{\partial t} + \hat{u}_r \frac{\partial \hat{u}_\theta}{\partial \hat{r}} + \frac{\hat{u}_\theta}{\hat{r}} \frac{\partial \hat{u}_\theta}{\partial \hat{\theta}} + \frac{\hat{u}_\theta \hat{u}_r}{\hat{r}} + \hat{u}_y \frac{\partial \hat{u}_\theta}{\partial \hat{y}} &= -\frac{1}{\hat{r}} \frac{\partial \hat{\psi}}{\partial \hat{\theta}} + \hat{\nu} \frac{\partial^2 \hat{u}_\theta}{\partial \hat{y}^2} - 2\hat{u}_r \Omega \\ 0 &= -\frac{\partial \hat{\psi}}{\partial \hat{y}} \end{aligned} \tag{110}$$

For exactly the same conditions, [9] made use of a set of boundary layer equations where both the Coriolis and Centrifugal terms where present in the $\hat{r}$- and $\hat{\theta}$-momentum equations respectively. The work of [10] on the other hand has the Centrifugal force only present in the $\hat{r}$-direction and the Coriolis force only in the $\hat{\theta}$-direction. The derivation above indicates that in pure rotation about the $\hat{y}$-axis, the Coriolis force is present in both the $\hat{r}$- and $\hat{\theta}$-directions, but it follows mathematically (and logically) that the centrifugal term should only be present in the $\hat{r}$-momentum equation.

6. Numerical Verification of Formulations

The open source code OpenFOAM was utilized as a platform for the non-inertial solver development and subsequent numerical analysis. Implementation of the solver is discussed in a manner that facilitates reproduction of the code. The theoretical formulation and numerical methods used in the subsequent analysis are provided to add to the reproducibility of results.

The case analysed is a laminar rotating disk (6). Analytical results are available from the literature ([12],[17]). This is compared with the steady state numerical results.

In the non-inertial frame the velocity is zero at the wall since no-slip conditions is assumed. The velocity profile further away from the wall increases

Figure 6: Graphical Representation of the Boundary Layer on a Rotating Disk

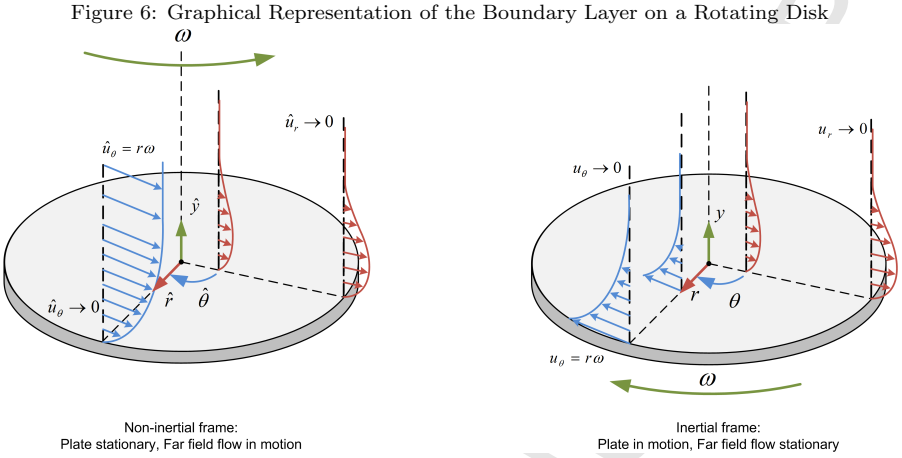

monotonically to approach the free-stream value in the far field. The free-stream value is dependant on the distance from the centre of rotation and the rotational velocity.

The boundary layer in the radial direction occurs as a result of secondary effects of due to tangential rotation. In an ideal flow u_r is zero through the entire domain. Viscous and secondary flow effects results in a boundary layer that is approaches zero velocity in the near-wall and far-field respectively. In the central regions of the boundary layer, the velocity profile is monotonically increasing closer to the wall, and monotonically decreasing closer to the boundary layer edge.

The boundary layer behaviour is discussed in terms of the boundary layer height, δ, displacement thickness, δ^*, momentum thickness, θ, and the Shape Factor, H (*Figure 7*).

The boundary layer height is the distance from the wall where the stream-wise velocity is 99% of the free stream velocity. The mathematical definitions of the displacement and momentum thickness are shown below.

$$\delta^* = \int_0^{y^* \to \infty} \left(1 - \frac{u}{U_\infty}\right) dy \tag{111}$$

Figure 7: Physical Interpretation of the Boundary Layer Parameters

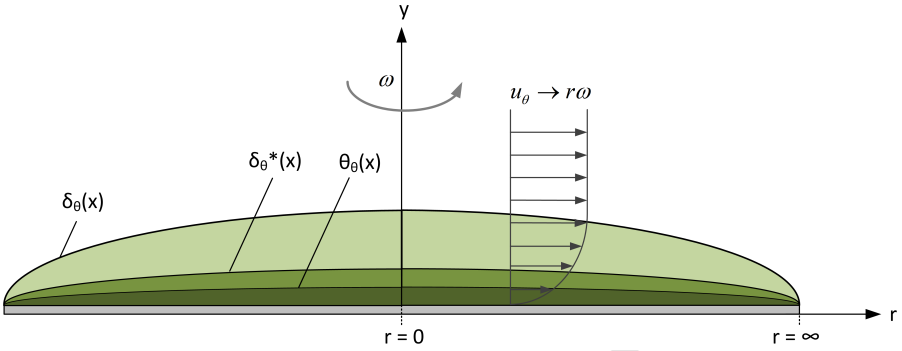

$$\theta = \int_0^{y^* \to \infty} \frac{u}{U_\infty}\left(1 - \frac{u}{U_\infty}\right) dy \tag{112}$$

A comparison of the parameters are shown in *Figure 8* . This indicates that the boundary layer thickness is be higher than the displacement thickness which in turn is be higher than the momentum thickness.

$$\delta > \delta^* > \theta \tag{113}$$

Figure 8: Comparison between the Boundary Layer, Displacement and Momentum Thicknesses

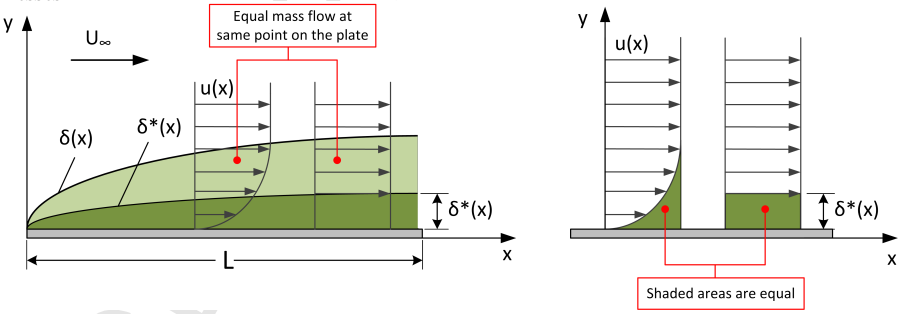

285 The parameters above are used to obtain a numerical approximation of the displacement and momentum thicknesses. The displacement thickness is the area under the $1 - \frac{u}{U_\infty}$ curve. The momentum thickness is the area under the $\frac{u}{U_\infty}(1 - \frac{u}{U_\infty})$ curve. This is demonstrated in *Figure 9*.

Figure 9: Boundary Layer Parameters on a Flat Surface

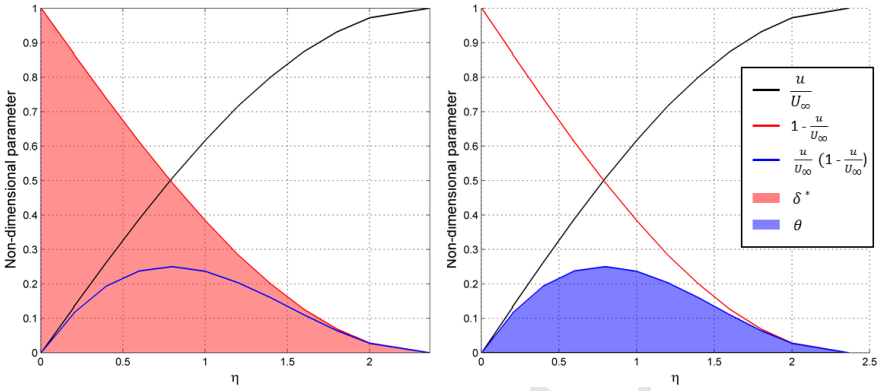

The Shape factor is determined from the displacement and momentum thicknesses.

$$H = \frac{\delta^*}{\theta} \tag{114}$$

6.1. Theoretical Formulation

The following assumptions were made with regards to the flow field:

- The flow can be completely described in the non-inertial reference frame.
- The fluid is Newtonian i.e. the viscous stresses in the fluid is linearly proportional to the strain rate.
- The ideal gas law is an appropriate equation of state to utilize as a closure model.
- The compressible form of the governing equations accurately describes the flow.
- The flow is well within the laminar regime, no turbulence models are employed.
- Viscous dissipation terms, $\hat{\phi}$, in the energy equation can be neglected since this is a laminar case and the dissipation term is associated with turbulent behaviour.

- The bulk viscosity is zero, as per Stoke's Law.
- Heat conduction is described by Fourier's Law.

The governing equations implemented in the code are *Equations 25, 15 and 35* respectively.

$$\hat{\nabla} \cdot \hat{\rho}\hat{\mathbf{u}} = 0 \tag{115}$$

$$\frac{\partial \hat{\mathbf{u}}}{\partial t} + (\hat{\mathbf{u}} \cdot \hat{\nabla})\hat{\mathbf{u}} = -\hat{\nabla}\hat{\psi} + \nu\hat{\nabla}^2\hat{\mathbf{u}} + \underbrace{2\hat{\mathbf{u}} \wedge \boldsymbol{\Omega}}_{\text{Coriolis}} \underbrace{- \hat{\mathbf{x}} \wedge \boldsymbol{\Omega} \wedge \boldsymbol{\Omega}}_{\text{Centrifugal}} \tag{116}$$

$$\frac{\partial \hat{\rho}\hat{e}}{\partial t} + (\hat{\nabla} \cdot \hat{\rho}\hat{e}\hat{\mathbf{u}}) = \hat{\nabla} \cdot (\hat{k}\hat{\nabla}\hat{T}) + \hat{\Phi}_I \tag{117}$$

The system of governing equations above requires additional equation to close the system of equations. An equation of state, transport model and thermodynamic model is required to ensure that for the number of unknowns, there are the same number of equations. This specifies the equation of the state, transport model and thermodynamic model.

The equation of state used in this case is the ideal gas law. This relates the pressure to the density, gas constant and temperature of the fluid.

$$p = \rho R T \tag{118}$$

The transport model makes use the equation below, where the Prandtl number is expressed as a ratio of viscous diffusion rate over the thermal diffusion rate:

$$P_r = \frac{C_p \mu}{\kappa} \tag{119}$$

In this implementation either the internal energy or enthalpy can be used to determine the temperature profile in the fluid.

The enthalpy is a function of internal energy and pressure.

$$h_s = e_s + \frac{p}{\rho} \tag{120}$$

This equation can be re-written to make the internal energy the subject of the equation. The known quantities in the flow is then used to model the internal energy.

$$\begin{aligned} e_s &= h_s - \frac{p}{\rho} \\ &= \int_{T_0}^{T} C_p T - \frac{r_u T_0}{M_w} \end{aligned} \tag{121}$$

The total enthalpy can also be expressed as the sum of the static enthalpy and the enthalpy of the dynamic pressure ([18]).

$$h_t = h_s + 0.5\mathbf{U} \cdot \mathbf{U} \tag{122}$$

The static enthalpy is replaced with known quantities in the flow, and the equation becomes:

$$h_t = \int_{T_0}^{T} C_p dT + 0.5\mathbf{U} \cdot \mathbf{U} \tag{123}$$

The solution algorithm that is used in the simulation is the Pressure Implicit Method with Splitting of operators, referred to as the PISO method. The method consist of one predictor and two corrector steps for each local iteration and was used in its standard implementation in openFOAM.

The openFOAM code allows for the separate discretization treatments of divergence, gradient and laplacian terms. Time integration was done using the implicit Euler method ([19, 20]). In the steady state solutions the Courant number was kept below 0.9 and in the accelerating and decelerating cases a constant time step was used since time accurate results were required. Discretization of the divergence terms were done using Gauss's theorem ([19, 20]) with a total variate diminishing (TVD) scheme. The gradient and laplacian term terms were both discretised with Gauss's theorem and a central differencing scheme ([19, 20]).

6.2. Case Setup

Computational grids are required with a sufficient amount of cells in the near-wall viscous region. In the near-wall region a sufficient resolution between

Figure 10: Computational Domain for the Rotating Disk

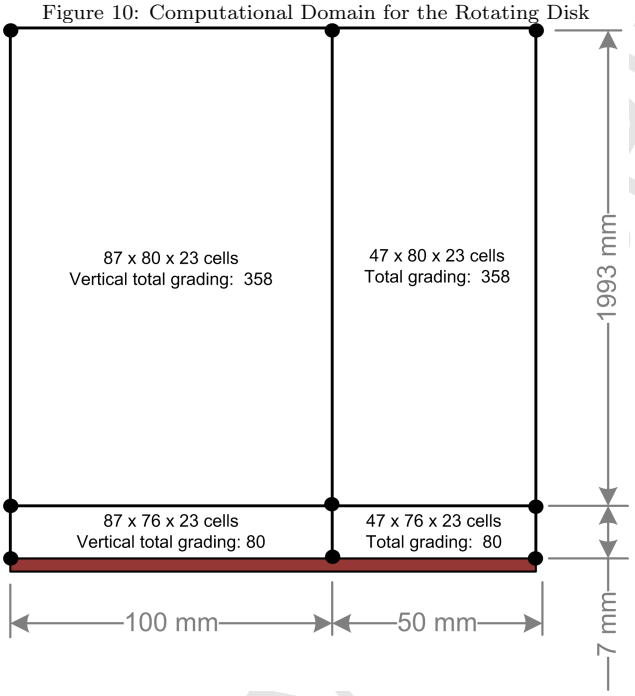

discrete points are required to obtain a solution that is representative on the flow. At least 15 cells are required in the boundary layer region on a steady solution to achieve this. Grids were generated with between 25 - 50 cells in the boundary layer (*Figure 10*). The first dimensionless cell node height is in the order of $y^+ = 1$ ([19]). Grids were designed according to these parameters.

$$y^+ = \frac{u^* y}{\nu} \approx 1 \tag{124}$$

The grids have been designed and tested to ensure grid independence. Results from the grid independence study is shown in *11* .

The boundary condition locations for the rotating disk are graphically represented in *Figure 12* . *Table 1* indicates the velocity, pressure and temperature boundary conditions.

The flow conditions were select to ensure that the fluid remains well within the laminar regime. To this effect the Reynolds number for a rotating disk must

Figure 11: Grid independence of the laminar rotating disk

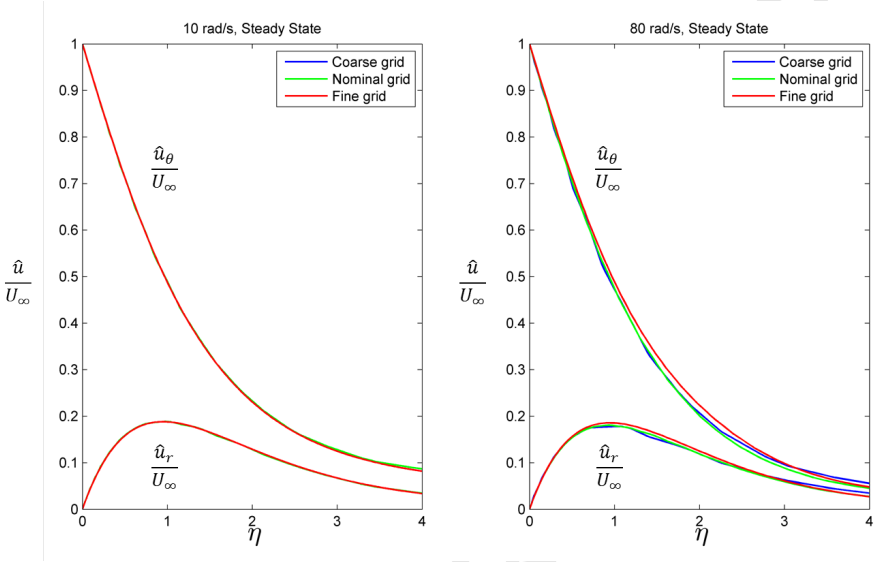

be below 500 ([21], [22]).

Table 2 shows the range of Reynolds numbers for each cases analysed.

Table 1: Boundary Conditions of the Rotating Disk

Boundary	Velocity	Pressure	Temperature
axis	symmetryPlane	symmetryPlane	symmetryPlane
bottomWall	no-slip wall	zeroGradient	zeroGradient
sidesLower	zeroGradient	zeroGradient	inletOutlet
sidesUpper	ARFFreeStreamVelocity	zeroGradient	inletOutlet
top	ARFFreeStreamVelocity	zeroGradient	inletOutlet
front/back	cyclic	cyclic	cyclic

$$Re_r = r\sqrt{\frac{\omega}{\nu}} \tag{125}$$

Figure 12: Graphical Representation of Rotating Disk Boundary Condition

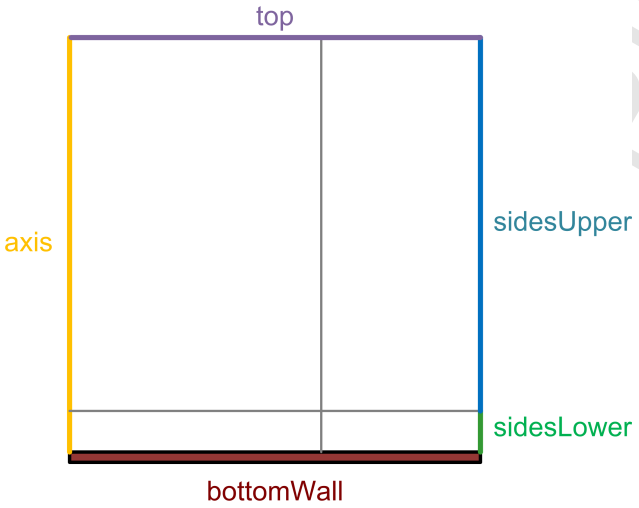

Table 2: Minimum and Maximum Reynolds Numbers of the Rotating Disk

Condition	$\omega[rad/s]$	Re_r	Re_{crit}
min	10	150	500
max	80	424.2	500

6.3. Results

In [12] a similarity solution is derived for the boundary layer on a rotating disk. This solution is discussed in detail by [13]. A solution is obtained by introducing a similarity variable, η, to the boundary layer equations (in cylindrical coordinates).

$$\eta = y\sqrt{\frac{\omega_y}{\nu}} \tag{126}$$

In the above equation y is the height normal to the wall, ω_y is the rotational velocity (in rad/s) about the y-axis and ν is the kinematic viscosity. Using this equation the partial differential equations (PDE) is reduced to a set of ordinary differential equations (ODE), as shown by [13]. This is solved numerically to obtain the velocity profiles.

Simulations were conducted for rotational velocities of 10 rad/s, 45 rad/s and

80 rad/s to obtain the steady state solution in the non-inertial frame (*Figures 13* and *15*). This solution was transformed to the inertial frame in order to compare it with the analytical result ([13, 12]) presented in *Figures 14* and *16*.

Figure 13: Non-Inertial Tangential Velocity Profiles

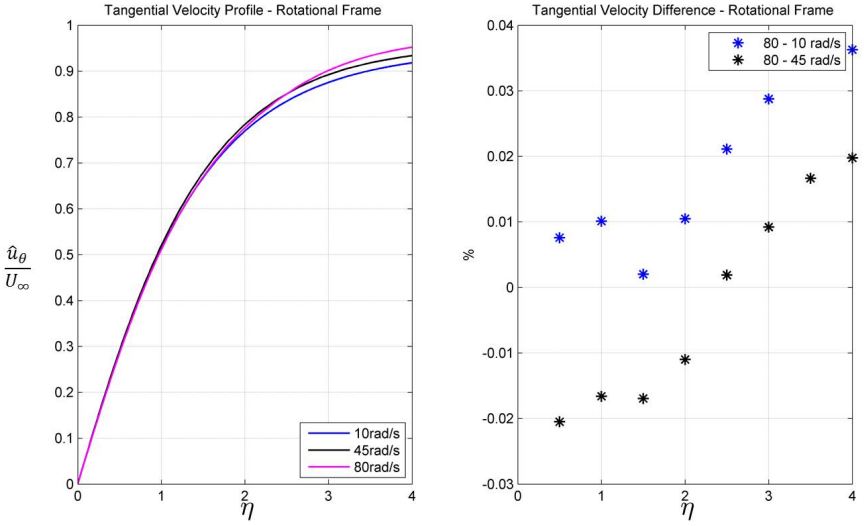

The tangential non-dimensional velocity profile is consistent with the analytical result near the wall region. Slight differences are observed in the far-field of the boundary layer. The non-dimensional value is slightly higher than the analytical value. This difference is increased with decreasing rotational velocity.

Similar behaviour is observed for in the radial direction. The radial non-dimensional velocity profile is overall consistent with the profile of the analytical result. The apex of the simulated curves are in the same order as the analytical apex. However, the simulated results are slightly higher than the analytical result.

The von Karman equations do not account for instabilities in the flow. The differences between the numerical and analytical results are due to the formation of laminar instabilities. Instabilities associated with rotating disks are mostly of Type I and Type II ([23], [24]). Type I instabilities occur due to inviscid

Figure 14: Comparison between Numerical and Analytical Tangential Velocity Results

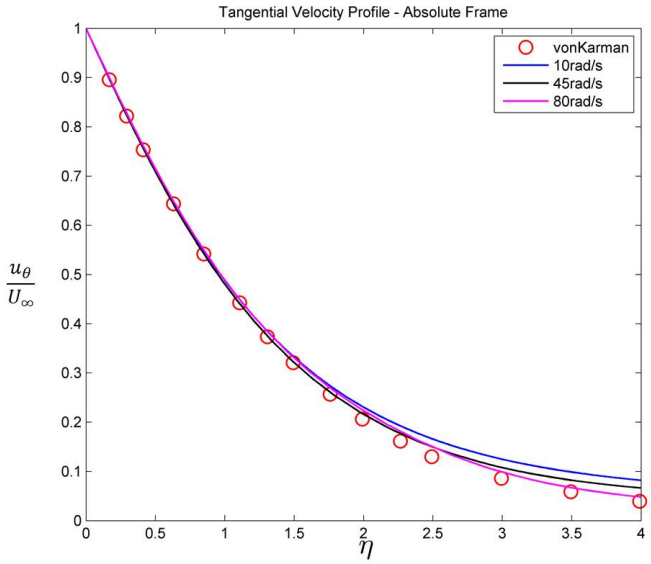

cross flow interactions. An example of Type I is the spiral vortices occurring above a Reynold number of 500. These vortices facilitates flow transition. Type II is instabilities that occur due to interaction between the Coriolis and viscous forces in the boundary layer. The differences observed here are due to cyclonic vortices at the centre of rotation. [25] investigated the sudden start of rotating disks. They experimentally observed the growth of the cyclonic vortices due to Ekman suction. It was noted that the growth rate of the vortices diminishes over time for steady state spin up conditions. This indicates that the cyclonic vortices are stationary in steady state conditions. This instability is classified as Type I since it operates in the inviscid region of the flow.

An increase in rotational velocity, adds to the momentum in the inviscid regions of the flow. The effect of the cyclonic vortice on the boundary layer are reduced since the increased momentum dominates the formation of cyclonic vortices. Therefore, with increasing rotational velocity, the cyclonic vortices decrease and the numerical solution approximates the von Karman solution.

Figure 15: Non-Inertial Radial Velocity Profiles

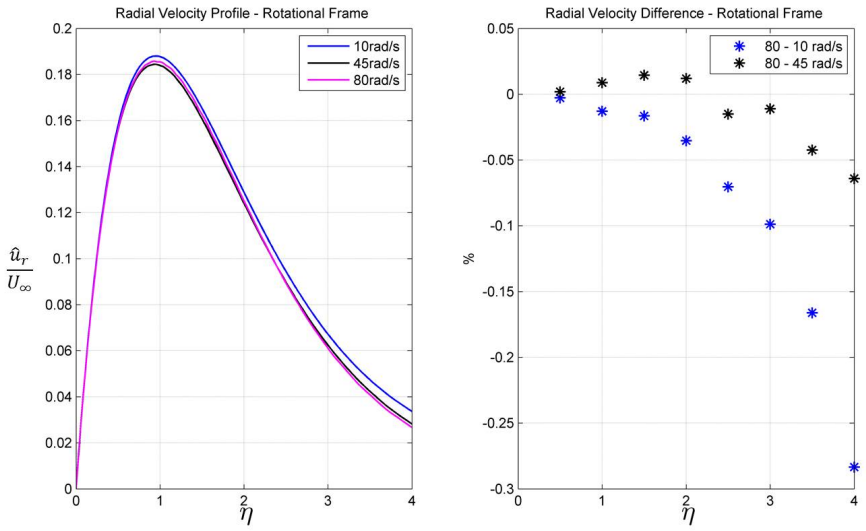

The boundary characteristic properties in the radial and tangential directions were determined for the numerical and analytical results.

$$\begin{matrix} \dfrac{\hat{u}_\theta}{U_\infty} \\ 1 - \dfrac{\hat{u}_\theta}{U_\infty} \\ \dfrac{\hat{u}_\theta}{U_\infty}(1 - \dfrac{\hat{u}_\theta}{U_\infty}) \end{matrix} \tag{127}$$

$$\begin{matrix} \dfrac{\hat{u}_r}{U_\infty} \\ 1 - \dfrac{\hat{u}_r}{U_\infty} \\ \dfrac{\hat{u}_r}{U_\infty}(1 - \dfrac{\hat{u}_r}{U_\infty}) \end{matrix} \tag{128}$$

The comparison of the boundary layer properties are shown in *Tables 3* and *4* for the tangential and radial direction respectively.

Comparisons are graphically represented for 10 rad/s and 80 rad/s in *Figures 17-20*. The effect of the cyclonic vortices on the boundary layer can be observed in the graphs. In the near wall regions deviation from the von Kar-

Figure 16: Comparison between Numerical and Analytical Radial Velocity Results

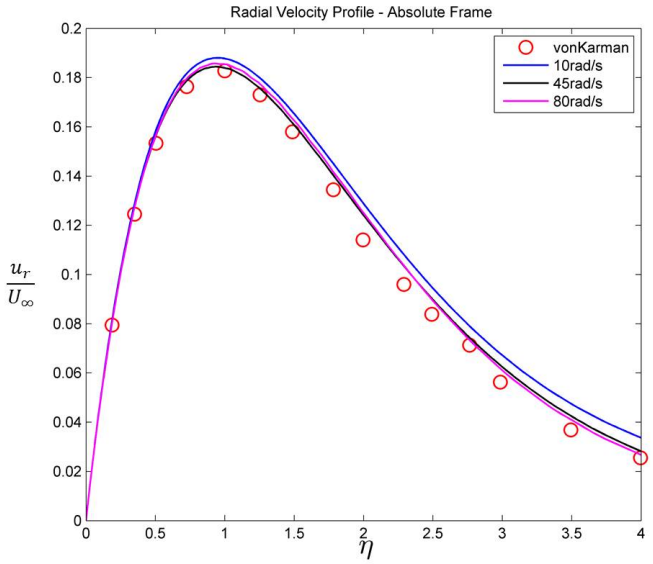

Table 3: Tangential Boundary Layer Properties of the Rotating Disk at 0.14 m radius

		δ_θ [m]	δ_θ^* [m]	θ_θ [m]	H_θ
10 rad/s	Analytical	$6.0e^{-3}$	$1.283e^{-3}$	$6.0102e^{-4}$	2.13
	Numerical	$6.2e^{-3}$	$1.475e^{-3}$	$7.5953e^{-4}$	1.94
	Difference %	3	15.01	26.37	-8.98
45 rad/s	Analytical	$2.8e^{-3}$	$6.0482e^{-4}$	$2.8332e^{-4}$	2.13
	Numerical	$2.83e^{-3}$	$6.5632e^{-4}$	$3.2964e^{-4}$	1.99
	Difference %	1.14	8.51	16.34	-6.73
80 rad/s	Analytical	$2.1e^{-3}$	$4.5362e^{-4}$	$2.1249e^{-4}$	2.13
	Numerical	$2.12e^{-3}$	$4.7743e^{-4}$	$2.2977e^{-4}$	2.07
	Difference %	1.05	5.25	8.13	-2.66

man results are small. The regions near the free-stream flow deviated from the analytical result. The deviation is indirectly proportional to rotational velocity.

Table 4: Radial Boundary Layer Properties of the Rotating Disk at 0.14 m radius

		δ_r [m]	δ_r^* [m]	θ_r [m]	H_r
10 rad/s	Analytical	$6.0e^{-3}$	$5.5865e^{-3}$	$3.6386e^{-4}$	15.35
	Numerical	$6.2e^{-3}$	$5.7001e^{-3}$	$4.2472e^{-4}$	13.42
	Difference %	3	2.03	16.72	-12.58
45 rad/s	Analytical	$2.8e^{-3}$	$2.6335e^{-3}$	$1.7152e^{-4}$	15.35
	Numerical	$2.83e^{-3}$	$2.6184e^{-3}$	$1.8724e^{-4}$	13.98
	Difference %	1.14	-0.57	9.16	-8.91
80 rad/s	Analytical	$2.1e^{-3}$	$1.9751e^{-3}$	$1.2864e^{-4}$	15.35
	Numerical	$2.12e^{-3}$	$1.9619e^{-3}$	$1.3964e^{-4}$	14.04
	Difference %	1.05	-0.66	8.55	-8.49

Figure 17: Comparison of Tangential Boundary Layer Characteristic Profiles for 10 rad/s

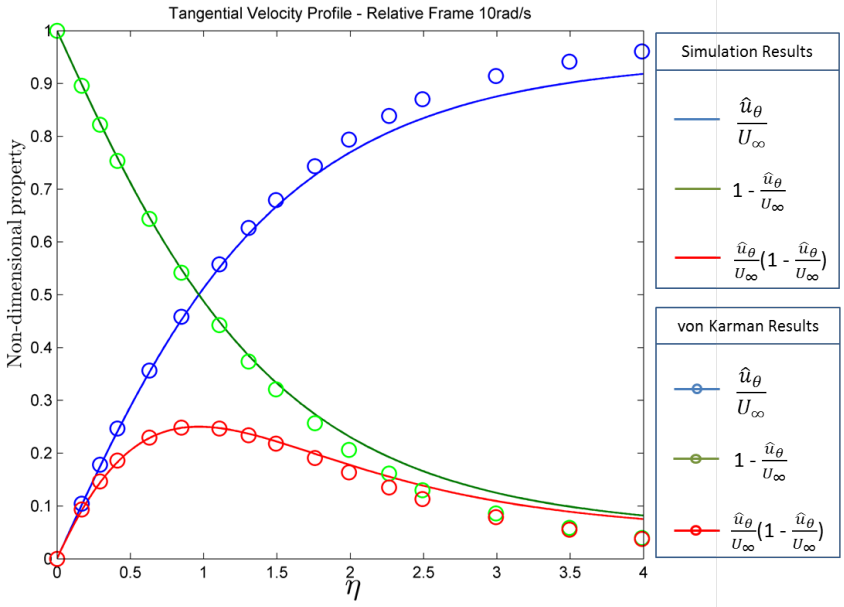

Figure 18: Comparison of Radial Boundary Layer Characteristic Profiles for 10 rad/s

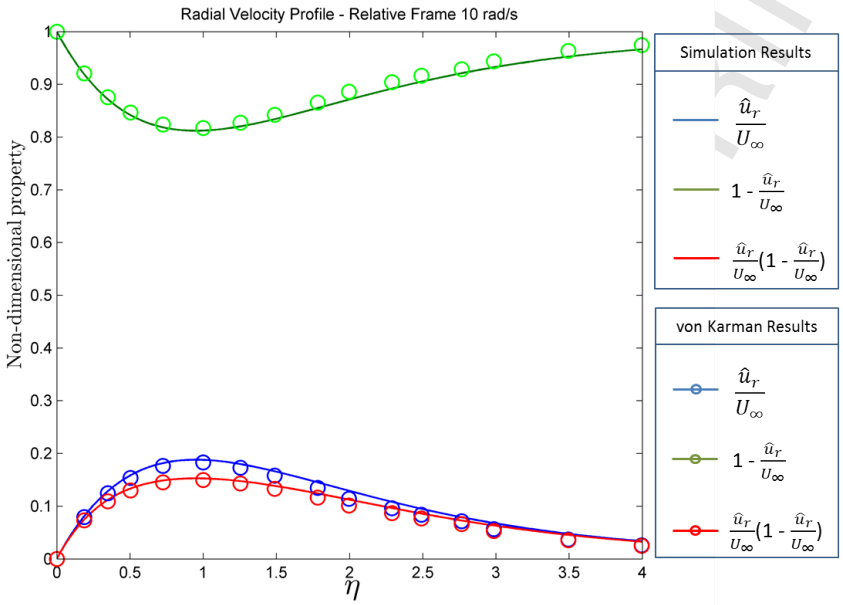

Figure 19: Comparison of Tangential Boundary Layer Characteristic Profiles for 80 rad/s

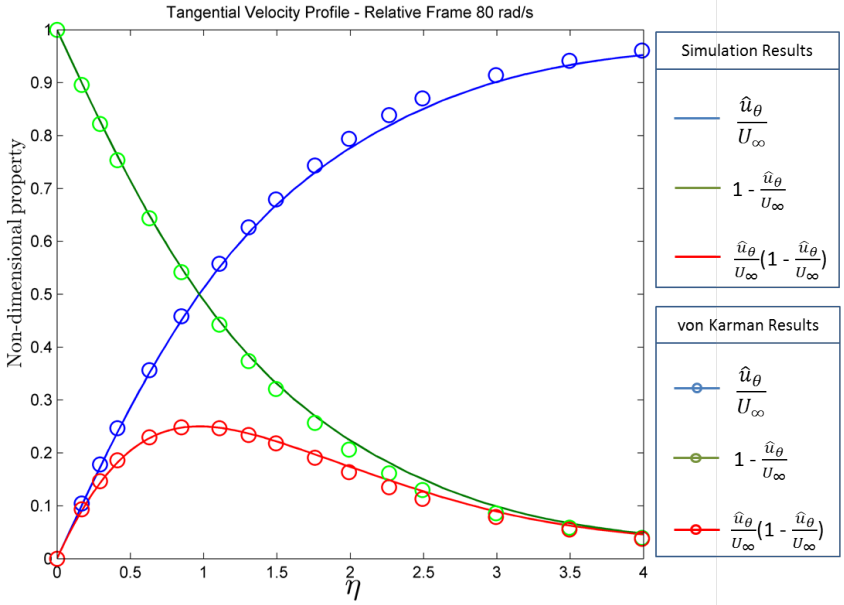

Figure 20: Comparison of Radial Boundary Layer Characteristic Profiles for 80 rad/s

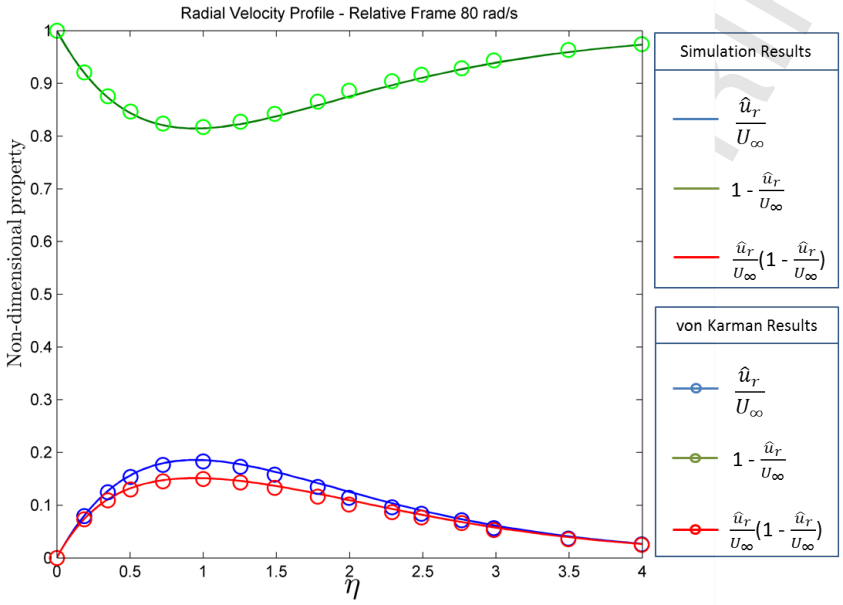

7. Conclusion

This paper presented an Eulerian derivation of the non-inertial Navier-Stokes equations for incompressible flow in constant rotational conditions. It further extends to derive the non-inertial boundary layer equations for flat plate and cone configurations.

It was shown that the continuity equation and the energy equation is invariant under transformation. Some instances have been observed in the literature where the fictitious effects were added to the energy equation due to misconception that arise when using the fluid parcel (Lagrangian) approach. This work indicates that no fictitious effects are present in the energy equation.

In the derivation of the non-inertial momentum equation the origin of the fictitious forces could be observed. The Coriolis force originates from the transformation of both the transient and the advection terms. The centrifugal force

originates from the transformation of the advection term.

The Eulerian approach does not allow for the misconceptions that can arise when using the Lagrangian approach. The method is mathematically rigorous, but more so the meaning of the terms is clear and leads to a improved understanding of the origin of the fictitious effects in the rotational frame.

The derived boundary layer equations are consistent with the equations available from the literature. Numerical solution of the boundary layer using a finite volume approach compared well with the analytical solution for a rotating disk.

Nomenclature

Super Scripts and Sub Scripts

$'$	Orientation preserving frame
$\hat{}$	Rotational frame
$\star$	Non-Dimensional quantity
rel	Relative conditions
t	Time
Δt	Change in time
y	projection on y-axis
z	projection on z-axis
∞	Free-stream conditions

Alphabet

$\mathbf{a}$	Acceleration vector
$\mathbf{b}$	Vector
e	Internal energy
k	Heat transfer coefficient
p	Pressure
r	Distance from axiz of rotation
t	Time

$\mathbf{u}$	Veloctiy vector
x	Distance in x-direction
$\mathbf{x}$	Position vector
y	Distance in y-direction
z	Distance in z-direction
G	Galilean operator
H	Shape factor
$\mathbf{I}$	Identity matrix
L	Characteristic length
O	Frame designations
R	Rotational transform operator
T	Temperature
U	Characteristic velocity
V	Velocity in x-direction
$\mathbf{V}$	Velocity vector
$\mathbf{X}$	Position vector

Greek Letters

β	Characteristic angle
δ	Boundary layer height
δ^*	Displacement thickness
ε	Pertubation parameter
θ	Momentum thickness
λ	Second viscosity
μ	Dynamic viscosity
ν	Kinematic viscosity
ρ	Density
ψ	Specific pressure $\frac{p}{\rho}$
Ω	Rotational speed around the z-axis
$\mathbf{\Omega}$	Rotational speed vector

Acknowledgment

The authors would like to convey their gratitude to the following person and institutions for their contributions towards this work:

1. Professor Akira Kageyama, Graduate School of System Informatics, Kobe University, Japan for his correspondence on his method.
2. Flamengro, a Division of Armscor SOC Ltd, South Africa
3. National Research Foundation of South Africa
4. Russian Foundation for Basic Research, Russian Federation

The data for this paper are available by contacting the corresponding author

References

[1] A. Kageyama, M. Hyodo, Eulerian derivation of the coriolis force, Geochemistry, Geophysics and Geosystems 7 (2) (2006) 1–5.

[2] A. Mager, Generalization of boundary-layer momentum-integral equations to three-dimensional flows including those of rotating systems, National Advisory Committee for Aeronautics Technical Report 1067.

[3] F. White, Viscous Fluid Flow, 2006.

[4] A. Gardi, Moving reference frame and arbitrary lagrangian eulerian approaches for the study of moving domains in typhon, Ph.D. thesis (2011).

[5] A. C. Limache, Aerodynamic modeling using computational fluid dynamics and sensitivity equations, Ph.D. thesis, Virginia Polytechnic Institute and State University (2000).
URL http://scholar.lib.vt.edu/theses/available/etd-04202000-14540007/

[6] V. Bogdanova, Universal equations of the laminar boundary layer on a rotating blade, Fluid Dynamics 6 (2) (1971) 251–259.

[7] H. Dwyer, Calculation of unsteady and three dimensional boundary layer flows, AIAA Journal 11 (6) (1973) 773–774.

[8] A. Mager, Three-dimensional laminar boundary layer with small cross flow, Journal of the Aeronautical Sciences 21 (12) (1954) 1.

[9] H. Dumitrescu, V. Cardos, A. Dumitrache, Modelling of inboard stall delay due to rotation, Journal of Physics: Conference Series 75.

[10] G. Martinez, J. Sorensen, W. Shen, Three-dimensional laminar boundary layer study on a rotating wind turbine blade, Journal of Physics: Conference Series 75.

[11] R. Diaz, W. Herrera, D. Manjarres, Work and energy in inertial and non inertial refernce frames, American Journal of Physics 77 (3) (2009) 270.

[12] T. von Karman, Uber laminare und turbulente reibung, Z. Angew. Math. Phys. 1 (1921) 233–252.

[13] H. Schlichting, Boundary-Layer Theory, 3rd Edition, McGraw-Hill, 1968.

[14] J. Tannehill, D. Anderson, R. Pletcher, Computational Fluid Mechanics and Heat Transfer, 1997.

[15] A. Mager, Laminar boundary layer problems associated with flow through turbomachines, Ph.D. thesis (1953).

[16] Anon, Navier-stokes equations presentation, Indian Institute of Technology Madras, CH2030 Momentum Transfer, Lecture Series url-http://www.che.iitm.ac.in/ srinivar/FM/ (2005).

[17] E. Sparrow, J. Greg, Mass transfer, flow and heat transfer about of rotating disk, Journal of Heat Transfer 82 (1960) 294–302.

[18] R. Sontagg, C. Borgnakke, Fundamentals of Thermodynamics, 1st Edition, Wiley and Sons Inc, 2001.

[19] J. Ferziger, M. Peric, Computational Methods for Fluid Dynamics, 3rd Edition, Springer, 2001.

[20] H. Versteeg, W. Malalasekera, An Introduction to Computational Fluid Mechanics, 1st Edition, Longman Scietific and Technical, 1995.

[21] S. Imayama, Studies of the rotating-disk boundary-layer flow, Technical Reports from the Royal Institute of Technology, Stockholm, Sweden, urlhttps://www.diva-portal.org/smash/get/diva2:781517/SUMMARY01.pdf (2014).

[22] P. Schmid, D. Henningson, Stability and Transition in Shear Flows, 1st Edition, Springer, 2001.

[23] S. Chefranov, Linear ekman friction in the mechanism of the cyclone-anticyclone vortex asymmetry and in a new theory of rotating super-fluid, A. M. Obukhov Institute of Atmospheric Physics RAS, Moscow, Russia, urlhttp://www.cardiometry.net/issues/no4-may-2014/new-theory-of-rotating-superfluid (2014).

[24] F. Zoueshtiagh, R. Ali, A. Colley, P. Thomas, P. Carpenter, Laminar-turbulent boundary-layer transition over a rough rotating disk, Journal of Fluid Mechanics 15 (8) (2003) 2441–2444.

[25] F. Moulin, J. Flór, On the spin-up by a rotating disk in a rotating stratified fluid, Journal of Fluid Mechanics 516 (2004) 155–180.

Appendix A

The inertial equation for incompressible momentum conservation is describe by the equation below:

$$\frac{\partial \mathbf{u}}{\partial t} + (\mathbf{u} \cdot \nabla)\mathbf{u} = -\nabla\psi + \nu\nabla^2\mathbf{u} \tag{129}$$

where

$$\psi = \frac{p}{\rho} \tag{130}$$

The first term that will be transformed to obtain an expression that relates the inertial to the rotational frame is the time dependant term. It will be done by finding an expression for the time derivative in the limit:

$$\frac{\partial \hat{\mathbf{u}}}{\partial t}(\hat{\mathbf{x}}_t, t) = \lim_{\Delta t \to 0} \frac{\hat{\mathbf{u}}(\hat{\mathbf{x}}_{t+\Delta t}, t + \Delta t) - \hat{\mathbf{u}}(\hat{\mathbf{x}}, t)}{\Delta t} \tag{131}$$

An expression for $\hat{\mathbf{u}}(\hat{\mathbf{x}}_{t+\Delta t}, t + \Delta t)$ must be found. The form that the expression must take, will directly relate the frames to each other:

$$\hat{\mathbf{u}}(\hat{\mathbf{x}}_{t+\Delta t}, t + \Delta t) = R^{\Omega(t+\Delta t)} G^{\mathbf{\Omega} \wedge \mathbf{x}_{t+\Delta t}}[\mathbf{u}(\mathbf{x}_{t+\Delta t}, t + \Delta t)] \tag{132}$$

The tools that is required to obtain an expression for the relation above is described in the derivation below.

Perform a Taylor series expansion for $\mathbf{x}_{t+\Delta t}$:

$$\mathbf{x}_{t+\Delta t} = \mathbf{x}_t + \Delta t\mathbf{V} + O(\Delta t^2) \tag{133}$$

The resulting series is truncated at the second order term and the derivative term is substituted through Equation 5. Re-arrangement of the terms will lead to an expression for displacement over the specific time interval:

$$\mathbf{x}_{t+\Delta t} - \mathbf{x}_t = \mathbf{x}_{\Delta t} = \Delta t(\mathbf{\Omega} \wedge \mathbf{x}) \tag{134}$$

A Taylor series expansion is done for $\mathbf{u}(\mathbf{x}_{t+\Delta t}, t+\Delta t)$, and with substitution of Equation 134 it results in:

$$\mathbf{u}(\mathbf{x}_{t+\Delta t}, t+\Delta t) = \mathbf{u}(\mathbf{x}_t, t) + [\Delta t(\mathbf{\Omega} \wedge \mathbf{x}) \cdot \nabla]\mathbf{u}(\mathbf{x}_t, t) + (\Delta t \frac{\partial}{\partial t})\mathbf{u}(\mathbf{x}_t, t) \quad (135)$$

Equation 135 is substituted into Equation 132 to get the expression:

$$\begin{aligned} \hat{\mathbf{u}}(\hat{\mathbf{x}}_{t+\Delta t}, t+\Delta t) &= R^{\Omega(t+\Delta t)} G^{\mathbf{\Omega} \wedge \mathbf{x}_{t+\Delta t}} \{\mathbf{u}(\mathbf{x}_t, t) + [\Delta t(\mathbf{\Omega} \wedge \mathbf{x}) \cdot \nabla]\mathbf{u}(\mathbf{x}_t, t) \\ &+ (\Delta t \frac{\partial}{\partial t})\mathbf{u}(\mathbf{x}_t, t)\} \end{aligned} \quad (136)$$

$G^{\mathbf{\Omega} \wedge \mathbf{x}_{t+\Delta t}}$ can be simplified as shown below if Equation 133 is substituted in the operator and truncated at the second order:

$$\begin{aligned} G^{\mathbf{\Omega} \wedge \mathbf{x}_{t+\Delta t}} &= G^{\mathbf{\Omega} \wedge \{\mathbf{x}_t + \Delta t[\mathbf{\Omega} \wedge \mathbf{x}_t + O(\Delta t^2)]\}} \\ &\approx G^{\mathbf{\Omega} \wedge \mathbf{x}_t} + G^{\mathbf{\Omega} \wedge (\Delta t \mathbf{\Omega} \wedge \mathbf{x}_t)} \end{aligned} \quad (137)$$

The expression for $\hat{\mathbf{u}}(\hat{\mathbf{x}}_{t+\Delta t}, t+\Delta t)$, then becomes:

$$\begin{aligned} \hat{\mathbf{u}}(\hat{\mathbf{x}}_{t+\Delta t}, t+\Delta t) &= R^{\Omega(t+\Delta t)}[G^{\mathbf{\Omega} \wedge \mathbf{x}_t} + G^{\mathbf{\Omega} \wedge (\Delta t \mathbf{\Omega} \wedge \mathbf{x}_t)}]\{\mathbf{u}(\mathbf{x}_t, t) \\ &+ [\Delta t(\mathbf{\Omega} \wedge \mathbf{x}) \cdot \nabla]\mathbf{u}(\mathbf{x}_t, t) + (\Delta t \frac{\partial}{\partial t})\mathbf{u}(\mathbf{x}_t, t)\} \end{aligned} \quad (138)$$

A final set of tools is required before the expressions for Equation 131 can be completed.

The assumption was made that point P is fixed in the rotating frame and the rotation is around the shared origin or the frames, then an expression can be derived for $\mathbf{x}_t$:

$$\begin{aligned} \hat{\mathbf{x}} &= R^{\Omega(t+\Delta t)}\mathbf{x}_{t+\Delta t} = R^{\Omega t}\mathbf{x}_t \\ \mathbf{x}_t &= R^{\Omega \Delta t}\mathbf{x}_{t+\Delta t} \end{aligned} \quad (139)$$

This relation is substituted in the Taylor series expansion for $\mathbf{x}_{t+\Delta t}$:

$$\begin{aligned}\mathbf{x}_{t+\Delta t} &= \mathbf{x}_t + \Delta t\mathbf{V} + O[\Delta t^2] \\ &= R^{\Omega\Delta t}\mathbf{x}_{t+\Delta t} + \Delta t(\mathbf{\Omega} \wedge \mathbf{x_t}) + O[\Delta t^2] \end{aligned} \tag{140}$$

Re-arrange this equation and consider in the limit as Δt approaches 0:

$$\lim_{\Delta t \to 0} \frac{R^{\Omega\Delta t}\mathbf{x}_{t+\Delta t} - \mathbf{x}_{t+\Delta t}}{\Delta t} = \lim_{\Delta t \to 0}(\mathbf{x}_t \wedge \mathbf{\Omega}) \tag{141}$$

Considering this relation for any vector $\mathbf{b}$, and take into account that $\mathbf{x}_{t+\Delta t} \to \mathbf{x}_t$ as $\Delta t \to 0$, the following equation is arrived at:

$$\lim_{\Delta t \to 0} \frac{R^{\Omega\Delta t}\mathbf{b} - \mathbf{b}}{\Delta t} = \mathbf{b} \wedge \mathbf{\Omega} \tag{142}$$

Substitute Equation 138 into Equation 131 to obtain the equation:

$$\begin{aligned}\frac{\partial \hat{\mathbf{u}}}{\partial t}(\hat{\mathbf{x}}_t, t) &= \lim_{\Delta t \to 0} \frac{R^{\Omega(t+\Delta t)}[G^{\mathbf{\Omega}\wedge\mathbf{x}_t} + G^{\mathbf{\Omega}\wedge(\Delta t\mathbf{\Omega}\wedge\mathbf{x}_t)}]\{[1 - \frac{1}{R^{\Omega\Delta t}} \\ &\quad \frac{+(\Delta t(\mathbf{\Omega} \wedge \mathbf{x}) \cdot \nabla)]\mathbf{u}(\mathbf{x}_t, t) + (\Delta t\frac{\partial}{\partial t})\mathbf{u}(\mathbf{x}_t, t)\}}{\Delta t} \end{aligned} \tag{143}$$

By using Equation 142, and after re-arrangement of the terms the following expression is arrived at:

$$\frac{\partial \hat{\mathbf{u}}}{\partial t}(\hat{\mathbf{x}}_t, t) = R^{\Omega t}[\frac{\partial}{\partial t} + (\mathbf{\Omega} \wedge \mathbf{x}) \cdot \nabla - \mathbf{\Omega}\wedge][G^{\mathbf{\Omega}\wedge\mathbf{x}}\mathbf{u}(\mathbf{x}_t, t)] \tag{144}$$

Substitute Equation 9 into the equation above will result in:

$$\begin{aligned}\frac{\partial \hat{\mathbf{u}}}{\partial t}(\hat{\mathbf{x}}_t, t) &= R^{\Omega t}[\frac{\partial}{\partial t} + (\mathbf{\Omega} \wedge \mathbf{x}) \cdot \nabla - \mathbf{\Omega}\wedge](\mathbf{u}(\mathbf{x}_t, t)) \\ &+ R^{\Omega t}[\frac{\partial}{\partial t} + (\mathbf{\Omega} \wedge \mathbf{x}) \cdot \nabla - \mathbf{\Omega}\wedge](\mathbf{x} \wedge \mathbf{\Omega}) \end{aligned} \tag{145}$$

In the equation above the transient component of $[\frac{\partial}{\partial t} + (\mathbf{\Omega}\wedge\mathbf{x})\cdot\nabla - \mathbf{\Omega}\wedge](\mathbf{x}\wedge\mathbf{\Omega})$ is equal to zero:

$$\frac{\partial}{\partial t}(\mathbf{x} \wedge \mathbf{\Omega}) = \frac{\partial \mathbf{x}}{\partial t} \wedge \mathbf{\Omega} + (\mathbf{x} \wedge \frac{\partial \mathbf{\Omega}}{\partial t}) = 0 \tag{146}$$

The first term is zero because the magnitude of $\mathbf{x}$ is constant over the time domain; its magnitude does not change with respect to the origin since this case involves pure rotation. The second term is zero due to constant rotation of the point P.

By introduction of the identity below, the terms $[(\boldsymbol{\Omega} \wedge \mathbf{x}) \cdot \nabla - \boldsymbol{\Omega}\wedge](\mathbf{x} \wedge \boldsymbol{\Omega})$ can be simplified:

$$(\mathbf{a} \cdot \nabla)(\mathbf{x} \wedge \boldsymbol{\Omega}) = \mathbf{a} \wedge \boldsymbol{\Omega} \tag{147}$$

The entire term is hence cancelled out:

$$\begin{aligned} [(\boldsymbol{\Omega} \wedge \mathbf{x}) \cdot \nabla - \boldsymbol{\Omega}\wedge](\mathbf{x} \wedge \boldsymbol{\Omega}) &= [(\boldsymbol{\Omega} \wedge \mathbf{x}) \cdot \nabla](\mathbf{x} \wedge \boldsymbol{\Omega}) - \boldsymbol{\Omega} \wedge (\mathbf{x} \wedge \boldsymbol{\Omega}) \\ &= \boldsymbol{\Omega} \wedge (\mathbf{x} \wedge \boldsymbol{\Omega}) - \boldsymbol{\Omega} \wedge (\mathbf{x} \wedge \boldsymbol{\Omega}) \\ &= 0 \end{aligned} \tag{148}$$

This leads to the final description of the unsteady terms in the momentum equation. Note the appearance of one part of the Coriolis effect manifesting in the relation below.

$$\frac{\partial \hat{\mathbf{u}}}{\partial t}(\hat{\mathbf{x}}_t, t) = R^{\Omega t}[\frac{\partial}{\partial t} + (\boldsymbol{\Omega} \wedge \mathbf{x}) \cdot \nabla - \boldsymbol{\Omega}\wedge](\mathbf{u}(\mathbf{x}_t, t)) \tag{149}$$

The relation of the inertial to the rotational advection term is described in the following manner:

$$(\hat{\mathbf{u}} \cdot \hat{\nabla})\hat{\mathbf{u}} = R^{\Omega t} G^{\boldsymbol{\Omega}\wedge\mathbf{x}}(\mathbf{u} \cdot \nabla)\mathbf{u} = R^{\Omega t}(G^{\boldsymbol{\Omega}\wedge\mathbf{x}}\mathbf{u} \cdot \nabla) G^{\boldsymbol{\Omega}\wedge\mathbf{x}}\mathbf{u} \tag{150}$$

Substitution of Equation 9 into the equation above results in:

$$\begin{aligned} (\hat{\mathbf{u}} \cdot \hat{\nabla})\hat{\mathbf{u}} &= R^{\Omega t}[(\mathbf{u} + \mathbf{x} \wedge \boldsymbol{\Omega}) \cdot \nabla](\mathbf{u} + \mathbf{x} \wedge \boldsymbol{\Omega}) \\ &= R^{\Omega t}[(\mathbf{u} + \mathbf{x} \wedge \boldsymbol{\Omega}) \cdot \nabla]\mathbf{u} + R^{\Omega t}[(\mathbf{u} + \mathbf{x} \wedge \boldsymbol{\Omega}) \cdot \nabla](\mathbf{x} \wedge \boldsymbol{\Omega}) \end{aligned} \tag{151}$$

Dividing out all the terms gives the final relation of the advection term between the frames. Note the appearance of the centrifugal effect and the other part of the Coriolis effect from the transformation of the advection term.

$$(\hat{\mathbf{u}} \cdot \hat{\nabla})\hat{\mathbf{u}} = R^{\Omega t}[(\mathbf{u} \cdot \nabla)\mathbf{u} + ((\mathbf{x} \wedge \boldsymbol{\Omega}) \cdot \nabla)\mathbf{u} + (\mathbf{u} \wedge \boldsymbol{\Omega}) + (\mathbf{x} \wedge \boldsymbol{\Omega}) \wedge \boldsymbol{\Omega}] \quad (152)$$

The gradient of the specific pressure term in the momentum equation is described between the frames in the following manner:

$$\hat{\nabla}\hat{\psi} = R^{\Omega t} G^{\boldsymbol{\Omega} \wedge \mathbf{x}} \nabla \psi \quad (153)$$

It was discussed earlier that scalars are invariant under the local Galilean transformation. Scalars will not be invariant under the rotational transform if spatial operations is performed on it since the axis along which the discretization is performed, changes between frames. The relation between the gradient of specific pressure in the inertial and rotational frames is therefore described by:

$$\hat{\nabla}\hat{\psi} = R^{\Omega t} \nabla \psi \quad (154)$$

The diffusion term in the inertial frame can be related to the rotational frame in the following manner:

$$\begin{aligned} \nu\hat{\nabla}^2\hat{\mathbf{u}} &= R^{\Omega t} G^{\boldsymbol{\Omega} \wedge \mathbf{x}} \nu \nabla^2 \mathbf{u} \\ &= R^{\Omega t} \nu \nabla^2 G^{\boldsymbol{\Omega} \wedge \mathbf{x}} \mathbf{u} \\ &= R^{\Omega t} \nu \nabla^2 (\mathbf{u} + \mathbf{x} \wedge \boldsymbol{\Omega}) \\ &= R^{\Omega t} \nu [\nabla^2 \mathbf{u} + \nabla^2 (\mathbf{x} \wedge \boldsymbol{\Omega})] \end{aligned} \quad (155)$$

If it is considered that:

$$\nabla^2 (\mathbf{x} \wedge \boldsymbol{\Omega}) = 0 \quad (156)$$

It can be shown that the diffusion term is invariant under constant transformation:

$$\nu\hat{\nabla}^2\hat{\mathbf{u}} = R^{\Omega t}\nu\nabla^2\mathbf{u} \tag{157}$$

Note that the pressure and viscous terms are Galilean invariant in this instance and combine the two components in a vector $\mathbf{f}(\mathbf{x},t)$:

$$\mathbf{f}(\mathbf{x},t) = -\nabla\psi + \nu\nabla^2\mathbf{u} \tag{158}$$

The new, combined parameter in the inertial and rotational frames is related in the following manner due to the invariance:

$$\hat{\mathbf{f}}(\hat{\mathbf{x}},t) = R^{\Omega t}\mathbf{f}(\mathbf{x},t) \tag{159}$$

The transformation of the momentum is completed through the summation of the unsteady and advection terms in the rotational and inertial frames as determined in Equation 149 and Equation 152:

$$\begin{aligned}\frac{\partial\hat{\mathbf{u}}}{\partial t} + (\hat{\mathbf{u}}\cdot\hat{\nabla})\hat{\mathbf{u}} &= R^{\Omega t}[\frac{\partial\mathbf{u}}{\partial t} + (\mathbf{u}\cdot\nabla)\mathbf{u} + 2\mathbf{u}\wedge\boldsymbol{\Omega} + \mathbf{x}\wedge\boldsymbol{\Omega}\wedge\boldsymbol{\Omega}] \\ &= R^{\Omega t}[\frac{\partial\mathbf{u}}{\partial t} + (\mathbf{u}\cdot\nabla)\mathbf{u}] + R^{\Omega t}[2\mathbf{u}\wedge\boldsymbol{\Omega} + \mathbf{x}\wedge\boldsymbol{\Omega}\wedge\boldsymbol{\Omega}]\end{aligned} \tag{160}$$

The first term grouping of the equation above is simplified as shown in the equations below. This was done using Equation 129, Equation 158 and Equation 159.

$$\begin{aligned}R^{\Omega t}[\frac{\partial\mathbf{u}}{\partial t} + (\mathbf{u}\cdot\nabla)\mathbf{u}] &= R^{\Omega t}[-\Delta\psi + \nu\nabla^2\mathbf{u}] \\ &= R^{\Omega t}\mathbf{f}(\mathbf{x},t) \\ &= \hat{\mathbf{f}}(\hat{\mathbf{x}},t)\end{aligned} \tag{161}$$

The second term grouping, with the insertion of Equation 9, becomes:

$$
\begin{aligned}
R^{\Omega t}[2\mathbf{u}\wedge\boldsymbol{\Omega}+\mathbf{x}\wedge\boldsymbol{\Omega}\wedge\boldsymbol{\Omega}] &= 2(R^{\Omega t}\mathbf{u})\wedge\boldsymbol{\Omega}+(R^{\Omega t}\mathbf{x})\wedge\boldsymbol{\Omega}\wedge\boldsymbol{\Omega} \\
&= 2[\hat{\mathbf{u}}-R^{\Omega t}(\mathbf{x}\wedge\boldsymbol{\Omega})]\wedge\boldsymbol{\Omega}+(R^{\Omega t}\mathbf{x})\wedge\boldsymbol{\Omega}\wedge\boldsymbol{\Omega} \\
&= 2\hat{\mathbf{u}}\wedge\boldsymbol{\Omega}-\hat{\mathbf{x}}\wedge\boldsymbol{\Omega}\wedge\boldsymbol{\Omega} \qquad (162)
\end{aligned}
$$

The two simplifications above is filled back into Equation 160 and results in the non-inertial momentum equation for constant rotation.

$$
\frac{\partial\hat{\mathbf{u}}}{\partial t}+(\hat{\mathbf{u}}\cdot\hat{\nabla})\hat{\mathbf{u}}=-\hat{\nabla}\hat{\psi}+\nu\hat{\nabla}^2\hat{\mathbf{u}}+2\hat{\mathbf{u}}\wedge\boldsymbol{\Omega}-\hat{\mathbf{x}}\wedge\boldsymbol{\Omega}\wedge\boldsymbol{\Omega} \qquad (163)
$$

It can be seen from the equation above that the fictitious forces associated with constant rotation is the centrifugal and the Coriolis effects. The centrifugal effect originates from the transformation of the advection terms while the Coriolis effect is form both the transient and advection terms.